Ebola virus antibody decay-stimulation in a high proportion of survivors

Charlene Adaken[1,2*], Janet T Scott[2,3,4*], Raman Sharma[5*], Robin Gopal[6], Steven Dicks[7,8], Saidia Niazi[7,8], Samreen Ijaz[7,8], Tansy Edwards[9], Catherine C Smith[3,10], Christine P Cole[11], Philip Kamara[12], Osman Kargbo[12], Heidi A Doughty[13,14], Johan van Griensven[15], Peter W Horby[16], Sahr M Gevao[12,17,], Foday Sahr[17,18], the Ebola-CP Consortium, Richard J Dimelow[19], Richard S Tedder[2,7,8,*], Malcolm G Semple[2,3,*], William A Paxton[1,2,*] and Georgios Pollakis[1,2,*@]

* Contributed equally

@ Corresponding Author

[1]Department of Clinical Infection, Microbiology and Immunology, Institute of Infection, Veterinary & Ecological Sciences, University of Liverpool, Liverpool, UK

[2]NIHR Health Protection Research Unit in Emerging and Zoonotic Infections (HPRU EZI), University of Liverpool Liverpool, UK

[3]Faculty of Health and Life Science, University of Liverpool, Liverpool, UK

[4]University of Glasgow-MRC Center for Virus Research, Glasgow, UK

[5]Department of Tropical Disease Biology, Liverpool School of Tropical Medicine, UK

[6]High Containment Microbiology, National Infections Service. Public Health England, UK

[7]Blood Borne Virus Unit, National Infection Service, Public Health England, London, UK

[8]Transfusion Microbiology, National Health Service Blood and Transplant, London, UK

[9]MRC Tropical Epidemiology Group, London School of Hygiene and Tropical Medicine, London, UK

[10]Travel Medicine and International Health Team, Health Protection Scotland, Glasgow, UK

[11]College of Medicine and Allied Health Sciences, Freetown, Sierra Leone

[12]National Safe Blood Service, Ministry of Health and Sanitation, Freetown, Sierra Leone

[13]National Health Service Blood and Transplant, Birmingham, UK

[14]College of Medical and Dental Sciences, University of Birmingham, Birmingham, UK

[15]Institute of Tropical Medicine, Antwerp, Belgium

[16]Centre for Tropical Medicine and Global Health, University of Oxford, Oxford, UK

[17]College of Medicine and Allied Health Sciences, University of Sierra Leone, Freetown, Sierra Leone

[18]34 Military Hospital, Republic of Sierra Leone Armed Forces, Freetown, Sierra Leone

[19]GlaxoSmithKline, Gunnels Wood Road, Stevenage, Herts, SG1 2NY

Abstract

Neutralizing antibody (nAb) function provides a foundation for vaccine and therapeutic efficacy[1-3]. Utilising a robust *in vitro* Ebola Virus (EBOV) pseudo-particle infection assay together with a well-defined set of solid phase assays we describe a wide spectrum of antibody responses in a cohort of healthy Ebola survivors from the Sierra Leone outbreak (2013-2016). Pseudo-particle virus (PPV) nAbs correlated with total anti-EBOV reactivity and nAbs against live EBOV. Variant EBOV glycoprotein (EBOV-GP) (1995 and 2014 strains) were found to be similarly neutralized. During longitudinal follow up antibody responses increased rapidly in a "decay-stimulation-decay" pattern suggesting *de novo* EBOV antigenic restimulation after recovery. A pharmacodynamic model of antibody reactivity identified a decay half-life of 77–100 days and a doubling-time of 46–86 days in a high proportion of survivors. The highest antibody reactivity was induced at around 200 days post-cure. The model suggests that EBOV antibody reactivity declines over 0.5-2 years post-cure. In a high proportion of healthy survivors' antibody responses undergo rapid re-stimulation. Vigilant follow up of survivors and possible elective *de-novo* antigenic stimulation by vaccine immunisation needs consideration to prevent EBOV viral recrudescence in recovering individuals to mitigate the potential risk to reseeding an outbreak.

Main

Limited Ebola virus (EBOV) outbreaks have been recorded since 1976[1]. The much larger 2013–2016 West African epidemic (28,610 cases), and the ongoing 2018 Eastern Zaire outbreak (3,188 cases as of September 2019) (https://www.who.int/emergencies/diseases/Ebola/drc-2019) in the Democratic Republic of Congo proved to be more extensive. The larger outbreaks have indicated viral persistence in some individuals with the potential for subsequent transmission of virus[2]. Due to limited EBOV outbreaks the understanding of natural induced immune responses is limited and vaccine induced correlates stem from animal models[3]. These models have indicated that total IgG binding antibody levels can correlate with protection along with neutralising antibody (nAb) responses, which can typically be low. Human outbreaks have provided valuable information regarding EBOV therapeutic[4] and vaccine intervention strategies[5-7]. More recently nAbs have been the focus of therapeutic development[8-12] where a cocktail of monoclonal antibodies (mAbs) was administered during the 2013-2016 outbreak[12-13] and with evidence of efficacy in trials conducted in the DRC[14]. In early 2015, two related studies [Ebola-Tx[15] and Ebola-CP[16]] were established where apparently health EBOV survivors were recruited with the intent of using their convalescent plasma (CP) to treat disease [4,16-17]. We used CP from the donors of the Ebola-CP study (**Supplementary Table 1a**) where samples were collected longitudinally (30-500 days) to better ascertain how nAb responses evolve. Such responses have previously been studied both in humans and primates with broad nAb activity[4,18-20].

A range of solid-phase enzyme-linked immunoassays (EIAs) based on Mayinga EBOV strain recombinant antigen were initially developed to characterise antibody responses in potential donors of therapeutic CP[21]. To circumvent the complexity of utilising replication competent EBOV in expanding the analysis to characterise neutralisation responses we utilised single-

round infectious pseudo-particle viruses (PVV) as described (see Methods). Optimal virus production and infectivity was identified by limiting dilution of EBOV14-GP expressing plasmid (**Extended Data Fig. 1a)**. GPs from three EBOV strains were used for PPV production; the early 2014 epidemic strain (pEBOV14-GP) (Accession: KP096421)[22], a modified variant (pEBOV14m-GP) comprising of mutations appearing early during the outbreak (**Fig. 1b, Supplementary Table 2**) and the 1995 Kikwit strain (pEBOV95-GP) (Accession: KC242799)[23] represented in the vaccine administered latterly in the 2013-2016 outbreak. EBOV14-GP PPV demonstrated consistently lower infectivity (**Fig. 1a**), presumably attributed to the T544I amino acid previously described[24]. The A82V alteration (pEBOV14m-GP) introduced early in the epidemic and subsequently found in more than 90% of the 2013-2016 isolates was also reported to have a higher infectivity profile[25]. Interestingly, this genotype did not associate with altered disease pathogenicity in a primate model system[26].

We utilized the above PPV infection assay in order to quantify nAb responses in CP donors (using limiting dilutions of plasma). In order to determine non-specific neutralisation effects we tested EBOV antibody negative plasmas (n=6) to find the range of non-specific inhibition (**Extended Data Fig. 1b**) and CPs with results subsequently falling within this range were considered lacking neutralizing potential. Furthermore, PPV expressing the HIV-1 envelope protein were used to test a high titre EBOV antibody positive plasma that was within the non-neutralizing range (**Extended Data Fig. 1b**). The WHO Anti-EBOV Convalescent Plasma International Reference Panel (NIBSC 16/344) was used to demonstrate the neutralizing potential of EBOV antibody-positive sera (IC_{50} range: 6.33-7.01 log_2 plasma dilution) (**Extended Data Fig. 1c**) which was found to be comparable to the values previously published[27]. The robustness of the assay was tested using EBOV survivors' plasma to inhibit

the three PPV strains produced, each in different batches with the assay repeated in two biologically independent experiments (**Extended Data Fig. 1d**).

CPs (n=52) demonstrated a wide range of neutralisation potential (**Supplementary Table 1b-d**), however had comparable profiles when assayed using all three EBOV PPV strains (**Extended Data Fig. 2a-c**). Half-maximal (IC_{50}) and seventy percent (IC_{70}) inhibitory concentrations determined correlated (**Extended Data Fig. 3**)**.** Within this cohort no differences in neutralizing titres were observed between the three virus strains (**Fig 1c, Extended Data Fig. 1e**)**.** pEBOV14-GP PPVs, demonstrating the lower infectivity profile (**Fig. 1a)**, did not differ from the pEBOV95-GP strain isolated twenty years earlier, or the pEBOV14m-GP strain carrying early epidemic mutations including the A82V variant associated with higher infectivity. However, individual CPs having high IC_{50} and IC_{70} values against one virus strain did not necessarily neutralize the other two (**Fig. 1d and Extended Data Fig. 1f**), potentially highlighting epitope diversity amongst individual participants as well as virus strains. A subset of donor CPs (n=5) with sequential samplings (totalling n=30) (**Supplementary Table 1e**) were assayed against the replication competent EBOV (RCE) Makona 2014 isolate. A significant correlation between the two neutralisation platforms was shown (**Fig. 1e and Extended Data Fig. 1g**) ($r=0.52$, $p<0.0001$). In addition, our neutralisation data demonstrated a similarly significant correlation with total anti-EBOV reactivity measured using the double antigen bridging assay (DABA) (**Fig. 1f**) ($r= 0.50$, $p<0.0001$, IC_{50}) and (**Extended Data Fig. 1h**) ($r= 0.55$, $p<0.0001$, IC_{70}) corroborating previous results[21] plus further validating our PPV neutralisation platform utilised here. The RCE and PPV assays demonstrated a stronger correlation when compared to neutralisation versus DABA. These two assays are targeting the same antibodies while DABA measures all antibodies and some

individuals would have differential responses, however, this was observed only in a very restricted number of donors.

While nAbs are thought to develop later in infection[28] our data demonstrates their presence as early as 30 days post-cure, also supporting previous studies[29-30] indicating that nAb levels are detectable and persist following viral clearance. Cross-sectional analysis of antibody responses did not indicate notable changes in titres during the observation window (~500 days) **(**IC_{50} /**Fig. 2a** and IC_{70} /**Fig. 2b),** comparable to the findings when fully replicating virus neutralisation was performed (**Fig. 2c).** However, within individuals often sustained decline was followed by a sharp antibody titre increase (**Fig. 2a-c)**.

The observed declines and subsequent rises in nAb levels identified in a portion of the study participants **(Fig. 2a-c**) indicates post-recovery *de novo* antigen stimulation. This was comprehensively demonstrated in Donor-CP-Pat-045 where antibody reactivity in all EIAs and including nAb initially decreased over a 45-day period (sampled six months post-recovery) prior to a sudden boost in antibody responses over a 23 day period (**Fig. 2d)**. It should be noted that all donors were tested for plasma EBOV RNA twice in Sierra Leone and shown to be aviraemic before discharge from Ebola Treatment Units. Furthermore, all samples received in the United Kingdom (UK) were subsequently re-tested upon arrival, providing evidence of no detectable viremia in the available samples taken in this observation period. Intriguingly, the increase in antibody reactivity was higher against EBOV95-GP than EBOV14-GP though participation in any vaccine study (where the immunogen would mimic the 1995 strain) was ruled out through self-reporting and later confirmed by the lead investigators of the two Ebola vaccine studies.

Following on from these observations Donor-CP-Pat-045 along with Donors-CP-Pat -018, -019, -021 and -049 were further tested using an additional panel of Enzyme Immune Assays (targeting the EBOV GP, nucleoprotein (NP) and VP40 matrix protein) and where similar variations in antibody responses were demonstrated (**Fig. 2e-f, Extended Data Fig. 4**) indicating that antibody re-stimulation targeted viral antigens which are not present in current vaccines and not just GP alone. Furthermore, similar variations in antibody responses were observed when implementing an IgG capture assay as well as a competitive antibody binding immunoassay, both targeting GP (**Extended Data Fig. 5**). Donor-CP-Pat -019 and -021 antibodies were also found to increase before subsequently decreasing. The increases in Donor-CP-Pat-045 EBOV antibodies occurred between mid-December 2015 and mid-January 2016. Two cases of Ebola were reported mid-January 2016 in the northern districts although Sierra Leone had been declared 'Ebola free' in November 2015 (https://www.theguardian.com/world/2015/sep/04/sierra-leone-village-in-quarantine-after-ebola-death. These donors and a control group of donors who did not demonstrate late rises in nAb reactivity were interviewed. All denied any intercurrent illness, known exposure to Ebola cases or participation in EBOV vaccine studies. It should also be borne in mind that by definition these convalescent donors had to meet individually the Sierra Leone National Safe Blood criteria for fitness to donate blood. Furthermore, interview and physical examinations were undertaken at each attendance for plasmapheresis. Whilst re-exposure to EBOV cannot be excluded it is assumed that the increase in antibody reactivity represents *de novo* antigenic stimulation at immune privileged sites boosting immunity. EBOV presence and ongoing replication in such sites has been described as late clinical recrudescence and reporting of sporadic viral transmission[31-36].

Given this high degree of intra-patient fluctuation in EBOV virus antibody responses we used the data available to develop compartmental population pharmacodynamic models to quantify antibody stimulation and decay trends in this cohort. The strong association between nAb and total antibody binding measured by DABA reactivity **(Fig 1f and Extended Data Fig. 1h)** enabled us to utilise the more replete DABA data set which incorporates extensive longitudinal time-points as described (**Supplementary Table 1f**) to perform model selection for stimulation and decay trends. The best fitting models for stimulation and decay were objectively identified. By comparison of the log-likelihood based AIC BIC metrics (**see methods and Supplementary Table 3a-c**) as a one compartment model with reduced stimulation at high antibody levels **(Fig. 3a)** and a two-compartment decay model with saturable recycling of antibody (**Fig. 3b**). The rate constant for stimulation for total antibody binding reactivity was found to be 0.03 day^{-1}, equivalent to a doubling time of 23 days (**Supplementary Table 4**) whilst the decay model provided a variable antibody concentration dependent rate constant equivalent to 30 days at half the maximum antibody level measured (**Supplementary Table 4**). The two best structural models as selected using the DABA data, were then fitted using the nAb titre values for the EBOV14-GP & EBOV95-GP strains and simulations performed **(Fig. 3e-h)**. The calculated stimulation rate constants for the virus strain variants were 0.067 day^{-1} and 0.046 day^{-1}, respectively, possibly reflecting variation in epitope targets. The calculated endogenous nAb decay rates were found to be similar for the different virus strains (0.025 day^{-1}/ EBOV14-GP and 0.025 day^{-1}/ EBOV95-GP) and matching the results initially found while modelling DABA reactivity (population mean of 0.028 day^{-1}) **(Supplementary Table 4**). Resultant concentration dependent half-lives at half maximal observed antibody levels were calculated to be 51 and 70 days for EBOV14-GP and EBOV95-GP, respectively. Interestingly, our findings are fully congruent with recent studies modelling endogenous antibody

metabolism[37]. To our knowledge this is the first population model of antibody level dynamics in EBOV survivors.

We next simulated the stimulation and decay profiles for 1000 EBOV survivors using the developed population models used (**Fig. 3c-3h**). The interquartile range of total antibody levels can be seen to vary widely for the simulated cohort when tracked longitudinally, indicating a wide-ranging array of doubling times/half-lives. The mean simulated doubling times were found to be 18.93 days [IQR: 11.68 -33.62], 10.36 days [IQR: 9.96-10.81] and 13.76 days [IQR: 9.52- 23.56], for total binding antibody, nAbs against EBOV14-GP and against EBOV95-GP respectively, indicating that overall EBOV14-GP was stimulated the fastest with the least variability, which is reasonable given this was the 2013-2016 epidemic strain. The median simulated endogenous decay half-lives were found to be 20.86 days [IQR:13.81-42.81], 27.40 days [IQR:19.62-41.66] and 28.23 days [IQR:24.33-33.33], respectively, in-line with previous estimates of IgG half-life[37].

Longitudinal analysis demonstrated increasing antibody reactivity in a high proportion of study participants, somewhere between 200 and 300 days, post-cure shown by DABA **(Fig 2e) (Extended Data Fig. 6),** blocking EIA (**Fig. 2e**) **(Extended Data Fig. 4),** IgG Capture and competitive EIA **(Extended Data Fig. 5)** as well as with antibody neutralisation measurements (**Fig. 2d**). This suggests that as antibody responses are waning antigen levels increase resulting in a boost to the residual primary antibody response. When comparing the lowest observed antibody titres after decline with the highest antibody titres following stimulation (prior to further *de novo* decline) we observe a statistical difference in antibody levels ($n=18$, $p<0.0014$) (**Extended Data Fig. 7**). We have simulated a typical decay-restimulation-decay profile based

on population median parameters and starting levels demonstrating a projected typical scenario in a substantial proportion of EBOV survivors. **(Fig. 3i)**.

Analyses of naturally occurring nAb responses in our EBOV CP donor cohort revealed a high degree of variation in strength and breadth of induced responses. Longitudinal analysis of B cell responses in EBOV infected individuals has revealed stark changes in immunoglobulin subclass switching, heightened alterations to hypermutations and naive B cell re-stimulations over time[38]. Our results would indicate that EBOV antigen re-exposure will be contributing to these observed alterations in antibody phenotypes described. It is encouraging to describe strong neutralisation cross-reactivity between EBOV strains representing outbreaks 20 years apart. This provides confidence that antibody induced either through natural infection or via a vaccine should elicit protection covering future outbreaks. Our results indicate that EBOV evolution[39-40], albeit slow, may result in altered neutralizing potential thus loss of vaccine efficacy **(Fig. 1c and Extended Data Fig. 1f)**. Furthermore, if CP possessing broadly neutralizing activity were to be used in therapeutic protocols then combining plasmas from several individuals may ensure a more successful outcome. The best option could be the preparation of a hyperimmune intravenous immunoglobulin blood product from a panel of donors rather than relying currently on the use of individually sourced components. The high frequency of *de novo* antigenic stimulation described within the cohort indicate a need for heightened surveillance of survivors to meet the potential clinical needs associated with virus recrudescence. Subclinical recrudescence may intensify the long-lasting post Ebola sequelae suffered by most EBOV survivors[41-42]. The cohort of CP donors studied here however represents a highly selected group of healthy individuals, further chosen through the use of field testing to have plasma antibody to EBOV in the upper quartiles of serological reactivity[21]. Therefore, they may represent convalescent individuals least likely to suffer viral

252 recrudescence. Occult virus persistence is therefore likely to be more frequent than previously
253 predicted, supporting findings that virus persists at sequestered sites in some individuals[2,43].
254 In a case study of an immunocompromised HIV-1 infected individual (CD4 cell count 46/μL)
255 EBOV could be detected in semen two years after the individual was discharged from the
256 treatment unit[37] further underlining the importance of immune-competence for EBOV
257 clearance. A longer and more frequent sampling would provide a more accurate indication of
258 the extend of Ab re-stimulation occurrence in these Ebola survivors.
259
260 The calculated mean half-life at median antibody levels has allowed predictions of time taken
261 to reach 95% depletion of any given level post antigenic stimulation and given the exponential
262 decay rate we can predict that the duration of six half-life periods (~180 to 417 days) will result
263 in depletion of antibody levels by >95%. As a result, protection of EBOV survivors from viral
264 recrudescence mediated by acquired immunity is likely to be 0.5-2 years post-recovery unless
265 boosted.
266
267 Continued surveillance of EBOV survivors is warranted considering the frequency of sub-
268 clinical *de-novo* antigenic stimulation we have described. Vaccination could be considered to
269 boost protective antibody responses in survivors. This would also have a particular role if
270 EBOV survivors are to be considered as plasma donors for use in future anti-Ebola passive
271 immunotherapy.
272

References

1. .Kasangye, K. A. et al. Historical Review of Ebola Outbreaks, Advances in Ebola Control, Samuel Ikwaras Okware, IntechOpen, https://www.intechopen.com/books/advances-in-Ebola-control/a-historical-review-of-Ebola-outbreaks
2. Heeney, J. L. Ebola: Hidden reservoirs. *Nature* **527**, 453-455 (2015).
3. Sullivan, N. J. Martin, J. E., Graham, B. S. & Nabel, G. J. Correlates of protective immunity for Ebola vaccines: implications for regulatory approval by the animal rule. *Nat. Rev. Microbiol*. **7**, 393-400 (2009).
4. Saphire, E. O. et al. Hemorrhagic Fever Immunotherapeutic Consortium. Systematic Analysis of Monoclonal Antibodies against Ebola Virus GP Defines Features that Contribute to Protection. *Cell* **174**, 938-952 (2018).
5. Henao-Restrepo, A. M. et al. Efficacy and effectiveness of an rVSV-vectored vaccine expressing Ebola surface glycoprotein: interim results from the Guinea ring vaccination cluster-randomised trial. *Lancet* **386**, 857-66 (2015).
6. Henao-Restrepo A.M. et al. Efficacy and effectiveness of an rVSV-vectored vaccine in preventing Ebola virus disease: final results from the Guinea ring vaccination, open-label, cluster-randomised trial (Ebola Ça Suffit!). *Lancet* **389**, 505-518 (2017).
7. Zhu, F. C. et al. Safety and immunogenicity of a recombinant adenovirus type-5 vector-based Ebola vaccine in healthy adults in Sierra Leone: a single-centre, randomised, double-blind, placebo-controlled, phase 2 trial. *Lancet* **389**, 621-628 (2017).
8. Ringe, R. & Bhattacharya. J. Preventive and therapeutic applications of neutralizing antibodies to Human Immunodeficiency Virus Type 1 (HIV-1*). Ther. Adv. Vaccines* **1**, 67-80 (2013).

9. Van Blargan, L. A., Goo, L. & Pierson, T.C. Deconstructing the Antiviral Neutralizing-Antibody Response: Implications for Vaccine Development and Immunity. *Microbiol. Mol. Biol. Rev*. **80**, 989-1010 (2016).
10. Crowe, J.E. Jr. Principles of Broad and Potent Antiviral Human Antibodies: Insights for Vaccine Design. *Cell Host Microbe* **22**, 193-206 (2017).
11. Garraud. O. Use of convalescent plasma in Ebola virus infection. *Transfus. Apher. Sci*. **56**, 31-34 (2017).
12. Zhang, Q. et al. Potent neutralizing monoclonal antibodies against Ebola virus infection. *Sci. Rep*. **6,** 25856 (2016).
13. King, L. B., West, B. R., Schendel, S.L. & Saphire E.O. The structural basis for filovirus neutralization by monoclonal antibodies. *Curr. Opin. Immunol*. **53**, 196-202 (2018).
14. Gaudinski, M. R. et al. VRC 608 Study team. Safety, tolerability, pharmacokinetics, and immunogenicity of the therapeutic monoclonal antibody mAb114 targeting Ebola virus glycoprotein (VRC 608): an open-label phase 1 study. *Lancet* **393**, 889-898 (2019).
15. van Griensven, J., Edwards, T. & Baize, S. Ebola-Tx Consortium. Efficacy of Convalescent Plasma in Relation to Dose of Ebola Virus Antibodies. *N. Engl. J. Med.* **375,** 2307-2309 (2016).
16. van Griensven, J. et al. The Use of Ebola Convalescent Plasma to Treat Ebola Virus Disease in Resource-Constrained Settings: A Perspective From the Field. *Clin. Infect. Dis*. **62**, 69-74 (2016).
17. Chippaux, J. P., Boyer, L. V. & Alagón, A. Post-exposure treatment of Ebola virus using passive immunotherapy: proposal for a new strategy. *J. Venom. Anim. Toxins Incl. Trop. Dis.* **21,** 3 (2015).
18. Wec, A. Z. et al. Development of a Human Antibody Cocktail that Deploys Multiple Functions to Confer Pan-Ebolavirus Protection. *Cell Host Microbe* **25**, 39-48 (2019).

19. Flyak, A. I. et al. Cross-Reactive and Potent Neutralizing Antibody Responses in Human Survivors of Natural Ebolavirus Infection. *Cell* **164**, 392-405 (2016).
20. Bramble, M.S. et al. Pan-Filovirus Serum Neutralizing Antibodies in a Subset of Congolese Ebolavirus Infection Survivors. *J. Infect. Dis*. **218**, 1929-1936 (2018).
21. Tedder, R. S. et al. Detection, characterization, and enrollment of donors of Ebola convalescent plasma in Sierra Leone. *Transfusion* **58**, 1289-1298 (2018).
22. Baize, S. et al. Emergence of Zaire Ebola virus disease in Guinea. *N. Engl. J. Med*. **371**, 1418-25 (2014).
23. Carroll, S. A. et al. Molecular evolution of viruses of the family Filoviridae based on 97 whole-genome sequences. *J. Virol*. **87**, 2608-16 (2013).
24. Hoffmann, M. et al. A Polymorphism within the Internal Fusion Loop of the Ebola Virus Glycoprotein Modulates Host Cell Entry. *J. Virol*. **91**, e00177-17 (2017).
25. Urbanowicz, R. A. et al. Human Adaptation of Ebola Virus during the West African Outbreak. *Cell* **167**, 1079-1087 (2016).
26. Marzi, A. et al. Recently identified mutations in the Ebola virus-Makona genome do not alter pathogenicity in animal models. *Cell. Rep*. **23**, 1806-1816 (2018).
27. Wilkinson, D. E. et al. Comparison of platform technologies for assaying antibody to Ebola virus. *Vaccine* **35**, 1347-1352 (2017).
28. Williamson L. E. et al. Early Human B Cell Response to Ebola Virus in Four U.S. Survivors of Infection. *J. Virol*. **93**, e01439-18 (2019).
29. Rimoin, A. W. et al. Ebola Virus Neutralizing Antibodies Detectable in Survivors of theYambuku, Zaire Outbreak 40 Years after Infection. *J. Infect. Dis*. **217**, 223-231 (2018).

30. Brown, J. F. et al. Anti-Ebola Virus Antibody Levels in Convalescent Plasma and Viral Load After Plasma Infusion in Patients With Ebola Virus Disease. *J. Infect. Dis*. **218,** 555-562 (2018).
31. Dokubo, E. K. et al. Persistence of Ebola virus after the end of widespread transmission in Liberia: an outbreak report. *Lancet Infect. Dis*. **18**, 1015-1024 (2018).
32. Subissi, L. et al. Transmission Caused by Persistently Infected Survivors of the 2014-2016 Outbreak in West Africa. *J. Infect. Dis*. **218**, S287-S291 (2018).
33. Shantha, J.G. et al. Ebola Virus Persistence in Ocular Tissues and Fluids (EVICT) Study: Reverse Transcription-Polymerase Chain Reaction and Cataract Surgery Outcomes of Ebola Survivors in Sierra Leone. *EBioMedicine*. **30**, 217-224 (2018).
34. Whitmer, S. L. M. et al. Ebola Virus Persistence Study Group. Active Ebola Virus Replication and Heterogeneous Evolutionary Rates in EVD Survivors. *Cell Rep*. **22**, 1159-1168 (2018).
35. Den Boon, S . et al. Ebola Virus Infection Associated with Transmission from Survivors. *Emerg. Infect. Dis*. **25**, 249-255 (2019).
36. Purpura, L.J. et al. Ebola Virus RNA in Semen from an HIV-Positive Survivor of Ebola. *Emerg. Infect. Dis.* **23**, 714-715 (2017).
37. Kendrick, F. et al. Analysis of a Compartmental Model of Endogenous Immunoglobulin G Metabolism with Application to Multiple Myeloma. *Front Physiol*. **8**, 149 (2017).
38. Davis C. W. et al. Longitudinal analysis of the human B Cell response to Ebola virus infection. *Cell* **177***,* 1566-1582 (2019).
39. Carroll, M. W. et al. Temporal and spatial analysis of the 2014-2015 Ebola virus outbreak in West Africa. *Nature*. **524**, 97-101 (2015).
40. Dudas, G. et al. Virus genomes reveal factors that spread and sustained the Ebola epidemic. *Nature* **544**, 309-315 (2017).

41. Scott, J.T., Sesay, F. R., Massaquoi, T. A., Idriss, B. R., Sahr, F. & Semple, M. G. Post-Ebola Syndrome, Sierra Leone. *Emerg. Infect. Dis*. **22**, 641-646 (2016).
42. Jagadesh, S. et al. Disability Among Ebola Survivors and Their Close Contacts in Sierra Leone: A Retrospective Case-Controlled Cohort Study. *Clin. Infect. Dis*. **66**, 131-133 (2018).
43. Rodger, J.M. *et al.* Late Ebola virus relapse causing meningoencephalitis: a case report. The Lancet **388** (10043) 498-503 (2016).

Figure legends

Fig 1: EBOV GP HIV-1 pseudo-typed virus neutralisation assay.. **(a)** Virus produced in 10 cm culture dishes (n=60), using 285 ng of pEBOV14-GP, pEBOV14m or pEBOV95 plasmids, the infectivity of virus from each plate assayed and plotted individually for the three virus strains produced (Data are presented as mean values of duplicate measurements. Kruskal-Wallis test was performed). **(b)** amino acid (aa) differences in the glycoproteins (yellow boxes) of the three virus isolates studied. The differences are found in the GP1 base (orange), GP1 head (blue), Glycan cap (purple), mainly in the Mucin like domain (green) and the fusion loop (red). The black bars above sequences indicate potential N-linked glycosylation site modifications. In pEBOV14m-GP the glycosylation at the 230 position site is lost. The colour code for the aa is indicated on the first line. **(c)** Neutralisation potential of CPs against three virus strains **(**pEBOV14-GP/n=98, pEBOV95-GP/n=80 and pEBOV14m-GP/n=79) expressed in IC_{50} (Data are presented as mean values of duplicate measurements. Kruskal-Wallis test was performed). **(d)** delta-IC_{50} neutralisation titres between virus strains pairs by each post-cure study participant. **(e)** Positive association between PPV IC_{50} titres the live virus plaque reduction neutralisation test (PRNT). **(f)** Positive association between PPV IC_{50} neutralisation titres and the double antigen bridging assay (DABA).

Fig.2: Convalescent neutralizing antibody titres. (a) nAb $IC_{50,}$ **(b)** nAb IC_{70} values against three PPV isolates; (EBOV14 (n=92), EBOV14m (n=70) and EBOV95 (n=76) followed over time. **(c)** nAb IC_{50} values against PRNT-EBOV14 (n=30) followed over time. In all three panels (2a, b and c) day 0 is defined as the day when virus PCR test became negative or when the individual was declared Ebola free and discharged from the Ebola Treatment Unit. Individual lines indicate individuals who has donated sequential plasma samples demonstrating non-canonical antibody titre variation. The black dotted lines are the 5-95 and 25-75 quartiles

and the red areas represent the 95% confidence intervals of the linear association (red solid line), that for PPV was calculated separately for each half of the observation period. **(d)** Longitudinal follow up of Donor-045. Longitudinal post-cure antibody variation of donor-045 demonstrated by PPV neutralisation of EBOV14 (light blue) and EBOV95 (dark blue) strains overlaid with virus neutralisation using the RCE PRNT (orange in upper panel) or total antibodies measured by DABA (green in lower panel). **(e-f)** Blocking EIAs using RCE were carried out for the detection of antibody against the Nucleoprotein [NP] (brown squares), the viral matrix protein 40 [VP40] (purple squares) and the Glycoprotein [GP] (green squares) using longitudinal plasma samples from donor-045 **(e)** and from donor-049 (**f**).

Fig. 3: Rates of EBOV antibody decay and recovery following the 2013-16 West Africa outbreak. (a) Schematic depicting the one compartment model for first order stimulation (based on a logistic growth model) and **(b)** schematic depiction of the two-compartment decay/metabolism of IgG with saturable recycling. **(c-h)** Mean antibody stimulation/decay 25^{th}, 50^{th} and 75^{th} percentile concentrations. Shaded bands indicate 95% CI of predicted percentiles. **(c-d)** total anti-EBOV reactivity as measured by DABA **(e-f)** neutralizing antibody titres against the EBOV14 virus strain and **(g-h)** neutralizing antibody titres against the EBOV95 Kikwit strain. Percentiles are calculated stimulation/decay profiles from Monte Carlo simulations of a population of 1000 randomly sampled individuals. Shaded areas surrounding percentile trajectories indicate 0.05 and 0.95 confidence intervals. (i) Graphic illustration of the post-infection acquired immune responses, illustrating the virus antigen stimulation hypothesis extrapolated from simulation of median fitted parameter values from the selected models. It depicts the acute sharp increase post-infection and the slow decrease post-cure. The observation period during this study is highlighted, demonstrating the antibody reactivity increase after

what is predicted to be a new antigenic stimulation occurring below a threshold of antibody protection.

METHODS

Ebola survivor cohort

Ebola virus disease survivors (N=115), previously described[42] with certificates (issued by Ebola Treatment Centers on discharge) were recruited as potential donors through 34 Military Hospital, Freetown, and the Sierra Leone Association of Ebola Survivors as participants in the study 'Convalescent plasma (CP) for early Ebola virus disease in Sierra Leone'. The study (ISRCTN13990511 & ACTR201602001355272) was approved by the Scientific Review Committee and Sierra Leone Ethics, authorised by the Pharmacy Board of Sierra Leone (PBSL/CTAN/MOHSCST001) and sponsored by the University of Liverpool.

Volunteers were considered suitable to donate plasma if they tested negative for blood borne infections (hepatitis B, hepatitis C, HIV, malaria and syphilis), had had 2 documented negative EBOV PCR tests 72 hours apart, had no acute febrile illness and had no comorbidity, such as heart failure, to suggest they might be at increased risk of adverse events during apheresis. Patients were not excluded if they exhibited indications of post Ebola syndrome (PES) (for example: musculoskeletal pain, headache, ocular problems) although such complaints were noted and subsequently contributed to the characterisation of PES[41-42, 44]. The majority of the participants were male (n=82), their age ranging between 18 and 52 with a median of 27 years old. The females' (n=32) age ranged between 18 and 42 with a median of 27 years (**Supplementary Table 1a**).

For transfusion safety reasons donor identity numbers were not confidential to donors during the conduct of the study; for the avoidance of doubt, donor identity numbers have since been dissociated. All participants (n=115) were tested using DABA, blocking EIA and IgG capture immunoassays[21]. PPV antibody neutralisation assays were performed with a subset of participants not selected on any criteria other than sample availability (N=52). The compartmental population pharmacodynamics model was developed on the more replete DABA dataset using those participants with longitudinal data (n=51) (**Supplementary Table 1f**).

Cell culture

HEK293T (ATCC® CRL-3216™) and TZM-bl[45-49] cells are adherent cell-lines cultivated in Dulbecco's modified eagle medium (Invitrogen: 12491-023), supplemented with 10% heat-treated foetal bovine serum (FBS) (Sigma: F7524), 2mM/ml L-glutamine (Invitrogen: 25030024), 100 U/ml penicillin (Invitrogen: 15140148) and 100 mg/ml streptomycin (Invitrogen: 15140148), referred to as complete DMEM (Thermofisher: 12491023). Cells were grown in a humidified atmosphere at 37ºC and 5% CO_2. Vero E6 cells (ECACC: 85020206) were grown in VP-SFM (Therno-Fisher: 11681-020).

EBOV PPV construct design

Three viral strain glycoprotein genes were cloned into pCDNA3.1 produced by GeneArt using gene synthesis. A 2014 isolate (KP096421)[22], a variant carrying the A82V, T230A, I371V, P375T, and T544I (**Fig. 1b**) identified by analysis of sequenced EBOV strains between March-August 2014[39] and the AY354458 1995 Kikwit isolate[50]. The later been used in ring vaccinations during the 2014 epidemic.

EBOV PPV production

We chose to utilise the HIV-1 SG3 ΔEnv and EBOV-GP expression plasmids, co-transfected into HEK293T cells, to generate infectious pseudo-particle virus (PPV) stocks[47,51-52]. The EBOV-GP-pseudo-typed lentiviral system generates single-cycle infectious viral particles. HEK293T cells were plated at a density of $1.2x10^6$ in a 10 cm diameter tissue culture dish (Corning: 430167) in 8ml of complete DMEM and incubated overnight. The cells were transfected with 2µg of pSG3Δenv along with 0.285µg of a plasmid expressing EBOV-GP using a cationic polymer transfection reagent (Polyethylenimine/polysciences: 23966-2), in the presence of OptiMEM (Invitrogen: 31985-070). OptiMEM was replaced 6 hrs post transfection with 8 ml of complete DMEM. 72 hours post-transfection supernatant containing the generated stock of single-cycle infectious EBOV-GP pseudo-typed virus particles were harvested, passed through a 0.45 µM filter and stored in aliquots at −80 °C. EBOV-GP plasmid (285 ng /10 cm culture dishes) was used to produce a large virus stock that was tested for infectivity (**Fig. 1a**) then pooled, aliquoted and stored under -80 °C.

EBOV PPV infection

EBOV infectivity was determined through infection of TZM-bl cell lines where luciferase activity (expressed from LTR promoter) is under the control of Tat expressed from the HIV-1 backbone. 100 µl of EBOV-GP virus was used to infect $1.5x10^4$ TZM-bl/ cells/ well for 6 hrs in a white 96 well plate (Corning: CLS3595). Following infection 150µl/well DMEM complete was added to the cells. 48 hrs post infection, media was discarded from the wells, cells were washed with phosphate buffered saline (PBS, Thernofisher:12899712), lysed with 30 µl Cell lysis buffer (Promega: E1531) and luciferase activity was determined by luciferase assay (Promega: E1501) using a BMGLabtech FluoroStar Omega luminometer. Negative controls

included pseudo-typed virus bearing no glycoproteins and TZM-bl cells alone which routinely resulted in luminescence of between 3000-7000 Relative Light Units (RLU).

EBOV PPV neutralisation

A panel of plasma samples (n= 52) from Ebola convalescent plasma and healthy blood donors (n= 6) were heat treated at 56ºC for 30 min and centrifuged for 15 mins, 13,000 RPM, aliquots were then stored at −80 °C. Plasma samples were serially diluted ½ with complete DMEM; 13 µl plasma dilution was incubated with 200 µl EBOV-GP PPV for 1 hr at RT. 100 µl of virus/plasma dilution was used to infect TZM-bl cells as described previously. Luciferase activity readings of neutralised virus were analysed i) by considering 0% inhibition as the infection values of the virus in the absence of convalescent plasma included in each experiment, ii) by considering 0% inhibition as the infection values of two consecutive high dilutions not inhibiting virus entry. Both methods produced highly correlated results (**Extended data Fig. 2d**) and the latter was used. The neutralisation potential of a CP was represented as the plasma dilution that reduced viral infectivity by 50% (IC_{50}) or by 70% (IC_{70}).

Enzyme Immune Assays

HIV-1-P24 capsid: Samples were diluted in 0.1% Empigen (Sigma: 30326)/ TBS prior to performing the ELISA assay (Fisher: 10167481). The p24 assays were conducted using the Aalto Bio Reagents Ltd protocol and recombinant p24 standard, p24 coating antibody (polyclonal sheep anti-HIV-1-p24 gag, Aalto Bio Reagents Ltd, D7320), secondary conjugate (alkaline phosphatase conjugate of mouse monoclonal anti-HIV-1-p24, Boehringer Mannheim, 1089-161) and ELISA light assay buffer. Plates were incubated 30 min at RT. prior to measuring luminescence with FLUOStar® Omega luminometer (BMG LabTech).

524 Double antigen bridging assay (DABA): Measured EBOV GP targeting antibody present in
525 Ebola survivor CP samples. EBOV GP antigen, Mayinga Zaire EBOV strain (IBT Bioservices:
526 0501-016) was pre-coated onto the 'solid phase', whilst a second antigen conjugated to
527 horseradish peroxidase (HRP) acted as the detector binding to EBOV antibody captured on the
528 solid-phase antigen in the first incubation step. Antibody reactivity was expressed as arbitrary
529 units/ml (au/ml) as compared to a standard; five reactive donor samples that were pooled and
530 attributed 1000 au/ml[21].
531
532 Blocking EIA: Antibody levels in CP to EBOV GP (glycoprotein), VP40, NP (nucleoprotein)
533 were determined by blocking of the binding of specific rabbit EBOV anti-peptide (GP, VP40,
534 NP) antibodies (IBT Bioservices) to EBOV Makona virion coated microplates. Microplate
535 wells were coated with 10,000-fold dilution of concentrated Ebola virions. EBOV patient CP
536 and negative control CP dilutions (1/100) were reacted on virion coated microplates for 4-6
537 hrs. CP dilutions were removed and plates were then reacted with EBOV anti-peptide
538 antibodies. Bound rabbit antibodies were detected by species specific horseradish peroxidase
539 conjugate (DAKO: P03991-2). Evidence of EBOV protein specific human antibodies in CP
540 was determined by the blocking of the binding of the antipeptide antibody compared to the
541 blocking of binding by the CP negative control. Results were expressed as a percentage of
542 blocking of the CP negative control reactivity.
543
544 IgG capture assay: IgG antibody present in CP was captured onto a solid phase coated with
545 rabbit hyperimmune anti-human γ-Fc and interrogated in a second incubation with HRP-
546 conjugated EBOV GP as above. Reactivity expressed as binding ratios derived as sample
547 OD/Cut off OD[21].
548

549 **Plaque Reduction Neutralization Test**

550 The wild type strain used for assays was EBOV Makona (GenBank accession number
551 KJ660347)[21], isolated from a female Guinean patient in March 2014 (virus provided to PHE
552 Porton by Stephan Günther, Bernhard-Nocht-Institute for Tropical Medicine, Hamburg,
553 Germany). The virus was propagated in Vero E6 cells and culture supernatant virions were
554 concentrated by ultracentrifugation through a 20% glycerol cushion; pellets resuspended in
555 sterile phosphate buffered saline at a titre of 10^9 focus forming units (FFU) per ml.

556

557 Wild type virus neutralising antibody titre in CP was determined by reacting serial dilutions of
558 CP with 100 FFU of EBOV virions for 1 hr at RT to allow antibody binding. EBOV virion CP
559 mixture was adsorbed to Vero E6 monolayers for 1 hr and then overlaid with cell growth
560 medium containing 1% (v/v) Avicel (Sigma-Aldrich). After 80-90 hrs EBOV foci were
561 visualised by immunostaining with anti-VLP (Zaire EBOV) antibodies (IBT Bioservices). All
562 work was undertaken under ACDP containment level 4 conditions.

563

564 **EBOV antibody decay and restimulation modelling**

565 Compartmental population analysis was performed to model the stimulation and decay of
566 antibody levels. All modelling and simulations were performed using Pmetrics version 1.4[53].
567 Within R version 3.2.2[54]. Antibody levels of EBOV survivors were sampled a different number
568 of instances, at varying intervals post convalescence due to follow-up adherence limitations in
569 the field. Different parts of decay/stimulation profiles were therefore captured with only a few
570 instances of contiguous decay-stimulation or stimulation-decay profiles being captured.
571 Stimulation and decay data were therefore modelled separately to most efficiently use the data.
572 Antibody stimulation/decay trends with ≥ 2 data points were including in population analysis
573 as this methodology has been proven to maximally use sparse clinical data with drug

development[55-56]. All points were plotted and visualised. An 'ascend' or a 'descend' was defined according to the prevailing trend. A 20% alteration in direction was tolerated as part of the prevailing ascend or descend as appropriate.

Structural model

Structural model selection was performed for the most replete DABA dataset. Model fitting and selection was performed using previously published protocols for fitting clinical datasets as described below[57-58]. Briefly, linear regression (intercept close to 0, slope close to 1) was used to assess the goodness-of-fit of the observed/predicted values, the coefficient of determination of the linear regression and minimisation of log-likelihood, (Akaike Information Criterion) AIC and (Bayesian information criterion) BIC values were used for model selection. A change in BIC drop of >2 is generally considered to be significant; with 2-6 indicating positive evidence, 2-6 indicating positive-to-strong evidence, 6-10 indicating strong evidence and >10 indicating very strong evidence[59].

Further details of this analysis leading to the choice of models and analysis of the fit of models to data can be found in **Supplementary Tables 3-4** and **Extended data Figures 8-9**.

All chosen structural models showed strong to very strong evidence of describing the data the best out of the compared models. Two structural models were tested for antibody stimulation, a 1-compartmental stimulation model and a 1-compartmental model with saturable stimulation, based on the logistic growth model. The logistic growth model framework allows for plateauing antibody levels observed for a subset of stimulation profiles. For antibody decay, four structural models were tested; a 1-compartment decay model with first order elimination, a 2-compartment decay model with first order elimination from the central compartment and

599 the above two structural models with saturable recycling offsetting the endogenous elimination
600 rate.
601
602 Antibody stimulation was best modelled using the 1-compartmental model with saturable
603 stimulation as described by Equation 1:
604
605 $$\frac{dX_1}{dt} = k_{growth}X_1\left(1 - \frac{X_1}{K_{max}}\right)$$ (Equation 1)
606
607 Where X_1, k_{growth} and K_{max} denoting antibody level in the compartment, the first order rate
608 constant for endogenous antibody stimulation and the maximal antibody level at which
609 stimulation plateaus, respectively.
610 For antibody decay, the two-compartment decay model with saturable FcRn-dependent
611 recycling (Equations. 2-4) as used to model antibody decay in multiple laboratory studies[37] was
612 found to best describe the data.
613 $$\frac{dX_1}{dt} = -k_{decay}X_1 - k_{cp}X_1 + k_{pc}X_2$$ (Equation 2)
614
615 $$\frac{dX_2}{dt} = k_{cp}X_1 - k_{pc}X_2$$ (Equation 3)
616
617 $$k_{decay} = k_{end} - \left(\frac{V_{max}}{X_1 + K_m}\right)$$ (Equation 4)
618
619 Where X_1 and X_2 are the antibody levels in the central and peripheral compartments. The rate
620 constants k_{decay}, k_{cp} and k_{pc} denote the empirically observed antibody level dependent rate
621 constant and the first order rate constants to and from the peripheral compartment. k_{decay} is in-
622 turn dependent on the endogenous decay rate k_{end} which is offset by a antibody dependent
623 saturable recycling rate described by a Michaelis-Menten term with parameters V_{max} and K_m
624 denoting the maximal recycling rate and antibody level at which half the maximal recycling

625 rate occurs. The optimal structural models above were then used to model the more sparse nAb
626 assay datasets allowing for comparability between DABA and nAb model parameters.
627 Generally, individual predicted vs. observed value correlations were found to excellent (R^2
628 >0.8) and population predictions vs. observed values were good (R^2 >0.6).
629
630 Monte Carlo simulations were performed using Pmetrics as previously described[57-58]. Briefly,
631 1000 individuals were randomly sampled from parameter distributions defined in the
632 population models of antibody stimulation and decay. The interquartile range of modelled
633 antibody levels was then plotted longitudinally for average starting antibody levels for decay
634 and stimulation profiles (**Fig. 3. c-h).**
635
636 With regard to the choice to model the stimulation and decay data separately: in principle, an
637 immune response followed by a gradual return to baseline post-stimulus could be characterised
638 by a single pharmacodynamic model. In the simplest form the dynamics can be described by a
639 single compartmental model with the stimulus placed on the input rate and first order
640 elimination, although more mechanistic models based on known pharmacology may also be
641 appropriate if the data is of sufficient quality to estimate the unknown model components. In a
642 controlled trial setting the onset of a stimulus event would be controlled and the subsequent
643 immune response measured relative to this origin with sufficient frequency to capture the
644 dynamics over time. In contrast, this study was observational with plasma samples taken
645 intermittently that captured only part of the changing levels in the nAbs – either the growth or
646 decay phase in most cases, but on occasion both. Given the lack of detectable viral load and
647 the observational nature of the nAb response data, the ability to fit a single, integrated
648 pharmacodynamic model to the data is limited. The most tractable solution in this case was to
649 split the data into two groups and modelled separately: the first model quantifying the rate of

increase in nAbs and the second model describing the subsequent decay. The antibody decay was based on[37]. Whilst this 2-stage approach did not allow data from the "stimulation" phase to inform the model fit of the "decay" phase – and vice versa , it did enable an accurate and quantitative characterisation of both the stimulation and decay dynamics, which has not been characterised for EBOV disease prior to this study, and which may be used to inform future work in this area and other impactful viral diseases such as COVID-19.

Statistical Analysis

Statistical analyses of data were implemented using GraphPad Prism 6.0 software. Unpaired sample comparisons were conducted for all data, however, individual figures state the corresponding statistical test performed. These include:

- Parametric and non-parametric t-tests (student t-test and Mann-Whitney U test)
- Parametric and non-parametric ANOVA (Ordinary ANOVA and Kruskal-Wallis test)

P values were depicted by *: * P value < 0.05, ** P value < 0.01, *** P value < 0.001, **** P value < 0.0001.

Data Availability

All datasets generated during and/or analysed during the current study are available from the corresponding authors on reasonable request.

References to the Methods

44. Scott, J.T. and M.G. Semple, Ebola virus disease sequelae: a challenge that is not going away. The Lancet Infectious Diseases, 2017. 17(5): p. 470-471.
45. Platt, E, J,, Bilska, M., Kozak, S.L., Kabat, D. & Montefiori, D. C. Evidence that ecotropic murine leukemia virus contamination in TZM-bl cells does not affect the outcome of neutralizing antibody assays with human immunodeficiency virus type 1. *J. Virol*. 2009 **83,** 8289-92 (2009).

677 46. Takeuchi, Y., McClure, M.O. & Pizzato. M. Identification of γ-retroviruses
678 constitutively released from cell lines used for HIV research. *J. Virol*. **82**, 12585-
679 1258 (2008).
680 47. Wei, X. et. al. Emergence of resistant human immunodeficiency virus type 1 in
681 patients receiving fusion inhibitor (T-20) monotherapy. *Antimicrob Agents*
682 *Chemother* **46**, 1896-1905 (2002).
683 48. Derdeyn, C.A. et.al. Sensitivity of human immunodeficiency virus type 1 to the
684 fusion inhibitor T-20 is modulated by coreceptor specificity defined by the V3 loop
685 of gp120. *J. Virol.* **74**, 8358-8367 (2000).
686 49. Platt, E.J., Wehrly, K,, Kuhmann, S.E., Chesebro, B. & Kabat, D. Effects of CCR5
687 and CD4 cell surface concentrations on infections by macrophagetropic isolates of
688 human immunodeficiency virus type 1**.** *J Virol* **72,** 2855-2864 (1998).
689 50. Biek, R., Walsh, P. D., Leroy, E. M. & Real, L. A. A Real Recent Common Ancestry
690 of Ebola Zaire Virus Found in a Bat Reservoir. *PLoS Pathog.* **2(10)**, e90 (2006).
691 51. Connor, R. I., Chen, B. K., Choe, S. & Landau N. R. Vpr is required for efficient
692 replication of human immunodeficiency virus type-1 in mononuclear phagocytes.
693 *Virology* **206**, 935–944 (1995).
694 52. Wei, X. et al. Antibody neutralization and escape by HIV-1. Nature **422**, 307-312
695 (2003).
696 53. Neely, M. N., van Guilder, M. G., Yamada, W. M., Schumitzky, A. & Jelliffe, R. W.
697 Accurate detection of outliers and subpopulations with Pmetrics, a nonparametric and
698 parametric pharmacometric modeling and simulation package for R. *Ther. Drug*
699 *Monit*. **34**, 467–476 (2012).
700 54. R: A language and environment statistical computing. v. 3.1.0 (R Foundation for
701 Statistical Computing, Vienna, Austria, 2014).
702 55. De Cock, R. F. W. et. al. Role of modelling and simulation in Paediatric Clinical
703 Research. *Eur J Clin Pharmacol*. **67,**S5–S16 (2011).
704 56. Aarons, L. et al. Role of Modelling and Simulation in Phase I Drug Development.
705 *Eur. J. Pharm. Sci.* **13**, 115-122 (2001).
706 57. Roberts, J. A. et al. Plasma and target-site subcutaneous tissue population
707 pharmacokinetics and dosing simulations of cefazolin in post-trauma critically ill
708 patients. *J. Antimicrob. Chemother.* **70**, 1495-1502 (2015).

58. Grau, S, et al. Plasma and peritoneal fluid population pharmacokinetics of micafungin in post-surgical patients with severe peritonitis. *J. Antimicrob. Chemother.* **70**, 2854–2861 (2015).
59. Mould, D. and R. Upton, *Basic Concepts in Population Modeling, Simulation, and Model-Based Drug Development—Part 2: Introduction to Pharmacokinetic Modeling Methods.* CPT: Pharmacometrics & Systems Pharmacology, 2013. **2**(4): p. 38.

Acknowledgements

We thank colleagues variously for their support and encouragement: the Sierra Leone Association of Ebola Survivors (Freetown, Sierra Leone); the members of the Convalescent Products and Allied Therapy Intervention Technical Committee; the Research Ethics Committee and the Pharmacy Board Committee (all Ministry of Health and Sanitation, Republic of Sierra Leone); staff in Virus Reference Department Public Health England (Colindale, England) for handling and clearing samples from quarantine; G. McCann and L. Matthews for project management (Institute of Translational Medicine and National Institute for Health Research Health Protection Research Unit in Emerging and Zoonotic Infections, University of Liverpool, Liverpool, UK); I. Bates' expertise in strengthening transfusion services (Department of International Public Health, Liverpool School of Tropical Medicine, Liverpool, UK); W.A. Brooks (International Severe Acute Respiratory and Emerging Infection Consortium [ISARIC], International Centre for Diarrheal Disease Research, Dhaka, Bangladesh, and Department of International Health, Johns Hopkins University, Baltimore, MD); M.P. Kieny (World Health Organization, Geneva, Switzer-land); C. Burm and D. Arango (Clinical Trials Unit, Institute of Tropical Medicine, Antwerp, Belgium); and N.F. Walker (London School of Hygiene and Tropical Medicine). Ashley Jones of the University of Liverpool; colleagues from the World Health Organization (WHO); and the International Severe Acute Respiratory and Emerging Infection Consortium (ISARIC). It is with affection

and sadness that we commemorate the passing on 5th July 2019 of Dr Samuel Baker, lately head National Safe Blood Service, Ministry of Health and Sanitation, Freetown, Sierra Leone. Proofreading support provided by Michel de Baar and graphical support provided by Suzanne Yee.

Author Contributions

GP, WAP, JTS and MGS initiated and designed the study. CA, RST, JTS, RJD and RG collected data and/or performed the analysis. CA, GP and WAP wrote the manuscript. MGS, JTS, GP, RST, RJD and WAP edited the manuscript. MGS sourced the funding and is Ebola-CP Consortium Lead Investigator. All authors were critical for study delivery whether through recruitment, coordination, collection of participant data & material, assay development or analysis of samples. All authors read and approved the contents of the manuscript. Readers are welcome to comment on the online version of the paper. GSK was not involved in the design, conduct or analysis of the study.

Competing interest declaration

All authors have no conflicts of interest to declare

Current affiliations

Richard S Tedder, Division of Infectious Diseases, Imperial College London, UK. Catherine C Smith, Oxford Vaccine Group, University of Oxford, Centre for Clinical Vaccinology and Tropical Medicine, Oxford, UK. Christine P Cole, Royal Liverpool and Broadgreen University Hospitals NHS Trust, Liverpool UK. Janet T Scott, MRC-University of Glasgow Centre for Virus Research, Glasgow UK.

762 **Consortia Authors**

763 The Consortium Investigators and Collaborators for Ebola CP (Convalescent Plasma for Early
764 Ebola Virus Disease in Sierra Leone) are: M.G. Semple (Consortium Lead Investigator) and
765 J.T. Scott, (both Faculty of Health and Life Science & NIHR Health Protection Research Unit
766 in Emerging and Zoonotic Infections University of Liverpool, Liverpool, UK); SM Gevao
767 (Country Lead Investigator), F. Sahr (Country Deputy Lead Investigator), C.P. Cole and J.
768 Russell (all College of Medicine and Allied Health Sciences, Freetown, Sierra Leone); S.
769 Baker, O. Kargbo, and P. Kamara (all National Safe Blood Service, Connaught Hospital,
770 Ministry of Health & Sanitation, Freetown, Sierra Leone); M. Lado and C.S. Brown (all King's
771 Sierra Leone Health Partnership, King's Health Partners & King's College London, London,
772 UK); B. Conton (Physio Fitness Rehabilitation Centre, Freetown, Sierra Leone); J. van
773 Griensven, R. Ravinetto and Y. Claeys (all Institute of Tropical Medicine, Antwerp, Belgium);
774 R.S. Tedder, R. Gopal, and T.J.G. Brooks (National Infection Service, Public Health England,
775 London, UK); C.C. Smith (Health Protection Scotland, UK); H.A. Doughty (NHS Blood and
776 Trans-plant & College of Medical and Dental Sciences, University of Birmingham,
777 Birmingham, UK); A. Mari Saez and M. Borchert (all Institute for Tropical Medicine and
778 International Health, Charité, Berlin, Germany); A.H. Kelly (Department of Sociology,
779 Philosophy and Anthropology, Exeter University, Exeter, UK); J.K. Baillie (The Roslin
780 Institute, University of Edinburgh, Edinburgh, UK); N. Shindo, and D. Pfeifer (all Department
781 of Pandemic and Epidemic Diseases, World Health Organization, Geneva, Switzerland); D.L.
782 Hoover (ClinicalRM Inc., Hinckley, OH); W.A. Fischer II and D.A. Wohl (all Department of
783 Medicine, University of North Carolina, Chapel Hill, NC); N.M. Thielman (Duke University
784 School of Medicine, Durham, NC); P.W. Horby and L. Merson (all Nuffield Department of
785 Medicine, University of Oxford, Oxford, UK); and P.G. Smith and T. Edwards (all Medical
786 Research Council Tropical Epidemiology Group, London School of Hygiene &Tropical

Medicine, London, UK). The authors alone are responsible for the views expressed in this work and they do not necessarily represent the views, decisions or policies of the institutions with which they are affiliated.

Funding

The study "Convalescent plasma for early Ebola virus disease in Sierra Leone (Ebola CP)" (ISRCTN13990511 and PACTR201602001355272) was supported by the Wellcome Trust (Award 106491) and Bill and Melinda Gates Foundation; Public Health England Ebola Emergency Response; and the Blood Safety Programme, National Health Service Blood and Transplant. JTS was supported by the Wellcome Trust. MGS and JTS were supported by the UK National Institute for Health Research Health Protection Research Unit in Emerging and Zoonotic Infections at the University of Liverpool. The funders had no role in the collection and analysis of the samples, in the interpretation of data, in writing the report, nor in the decision to submit the paper for publication.

Additional Information

Supplementary information is available for this paper.

Correspondence and requests for materials should be addressed to GP (g.pollakis@liverpool.ac.uk).

Extended Data Figure legends

Extended Data Fig. 1. (a) Variant pEBOV14-GP plasmid concentrations were transfected alongside 2000 ng of pSG3-HIV-1 backbone. The resulting pseudo-typed virus, quantified by a HIV-1-p24 capsid ELISA (squares), was tested for infectivity in TZM-bl cells as measured by luciferase activity (bars/mean value +-SD). The red marked square identifies the

glycoprotein concentrations that can be used in the assay. **(b)** Inhibition profiles with negative plasma donated from six individuals (grey squares), indicating no specific plasma inhibition during the neutralisation assay. All negative assays and plasmas were combined to define the range within which negative plasma control were acceptable (red squares) thus defining a valid assay. The blue line shows the lack of reactivity on the HIV-1-enveloped pseudo-typed virus by EBOV neutralizing convalescent plasma (CP) (squares and circles indicate the median and the vertical lines the standard error). **(c)** Neutralisation profiles of pEBOV14-GP by the WHO reference panel of anti-EBOV CP. The standard identifiers are shown. **(d)** Reproducibility of the neutralisation assay determined by measuring the IC_{50} of CP plasma on the three EBOV isolates (yellow-pEBOV14-GP, purple- pEBOV95-GP and green- pEBOV14m-GP). The two-tailed parametric paired t test was used. **(e)** Neutralisation potential of CPs against three virus strains **(**pEBOV14-GP/n=83, pEBOV95-GP/n=69 and pEBOV14m-GP/n=77) expressed in IC_{70} (Data are presented as mean values +/- SD. Kruskal-Wallis test was performed). **(f)** delta-IC_{70} neutralisation titres between virus strains pairs by each post-cure study participant. **(g)** Positive association between PPV IC_{70} titres the live virus plaque reduction neutralisation test (PRNT). **(h)** Positive association between PPV IC_{70} neutralisation titres and the double antigen bridging assay (DABA).

Extended Data Fig. 2. (a) anti-EBOV14-GP (n=92), **(b)** anti-EBOV14m-GP (n=70) and **(c)** anti-EBOV95-GP (n=76) neutralisation curves using serial dilutions of CP inhibiting PPV cell entry, as described in methods. The plasma samples were deciphered as possessing low (blue), intermediate (magenta) or high (orange) neutralisation to demonstrate the similar profiles of the three virus glycoproteins studied. The red square curve indicates the range of inhibition by control plasma. **(d)** Comparison of the analyses (n=30) ***i)*** considering the 0% inhibition value whenever two reciprocal consecutive high plasma dilutions produced equal infection levels ***ii)***

837 considering 0% inhibition as the infection values of virus in the absence of convalescent plasma
838 performed in each individual experiment. The Pearson correlation coefficients were computed.
839
840 **Extended Data Fig. 3.** Association of IC_{50} and IC_{70} neutralizing dilutions of the post-cure
841 plasma samples inhibiting cell entry of pseudo-typed virus particles harbouring the variant
842 EBOV GP molecules. The Pearson correlation coefficients were computed.
843
844 **Extended Data Fig. 4.** Longitudinal post convalescence nAb variation in the plasma of
845 individuals 18,19 and 21 demonstrated by pseudo-typed virus particle neutralisation. Anti-
846 EBOV14-GP (light blue) and anti- EBOV95-GP (dark blue) nAb titres were overlaid with the
847 blocking EIAs carried out for the detection of antibody against the Nucleoprotein [NP] (brown
848 squares), the viral matrix protein 40 [VP40] (purple squares) and the Glycoprotein [GP] (green
849 squares)
850
851 **Extended Data Fig. 5.** Longitudinal G-capture (pink) and competitive (green) EIAs performed
852 using the plasma individuals 18, 19, 21, 45 and 49 against the Glycoprotein as described in
853 Tedder et.al.[21] The antibody reactivities were overlaid with pseudo-typed virus particle IC_{50}
854 neutralisation values against EBOV14-GP (light blue) and EBOV95-GP (dark blue).
855
856 **Extended Data Fig. 6.** Total antibody reactivity as measured by double antigen bridging assay
857 (DABA)(average of a duplicate measurement) for the Ebola post-cure cohort participants with
858 longitudinal follow up (≥2 data points, n=51) demonstrating decline/re-stimulation/decline (in
859 any order) of antibody reactivity over-time. Decline is indicated by a black line and re-
860 stimulation by a yellow horizontal line.
861

Extended Data Fig. 7. Total antibody reactivity as measured by double antigen bridging assay (DABA). 'Lowest titre following decline' is the last point in a participant presenting antibody titres decline while 'High titre upon stimulation' is the subsequent point demonstrating antibody stimulation, Two-tailed parametric paired t-test (p=0.0014).

Extended Data Fig. 8. Observed versus predicted plots for selected logistic growth model for antibody stimulation, as determined by the DABA assay: (**a**) population predicted values (**b**) individual predicted values. Observed versus predicted plots for selected 2 compartment decay model with saturable recycling for antibody stimulation, as determined by the DABA assay: (**c**) population predicted values (**d**) individual predicted values. Solid red circles represent the individual observed/model-predicted Ab values. Solid blue line and dotted red line represents the line of regression and line of unity, respectively.

Extended Data Fig. 9 Flow diagram describing the observed antibody decrease and increase events as measured by DABA, which are used to develop the compartmental population pharmacodynamic models.

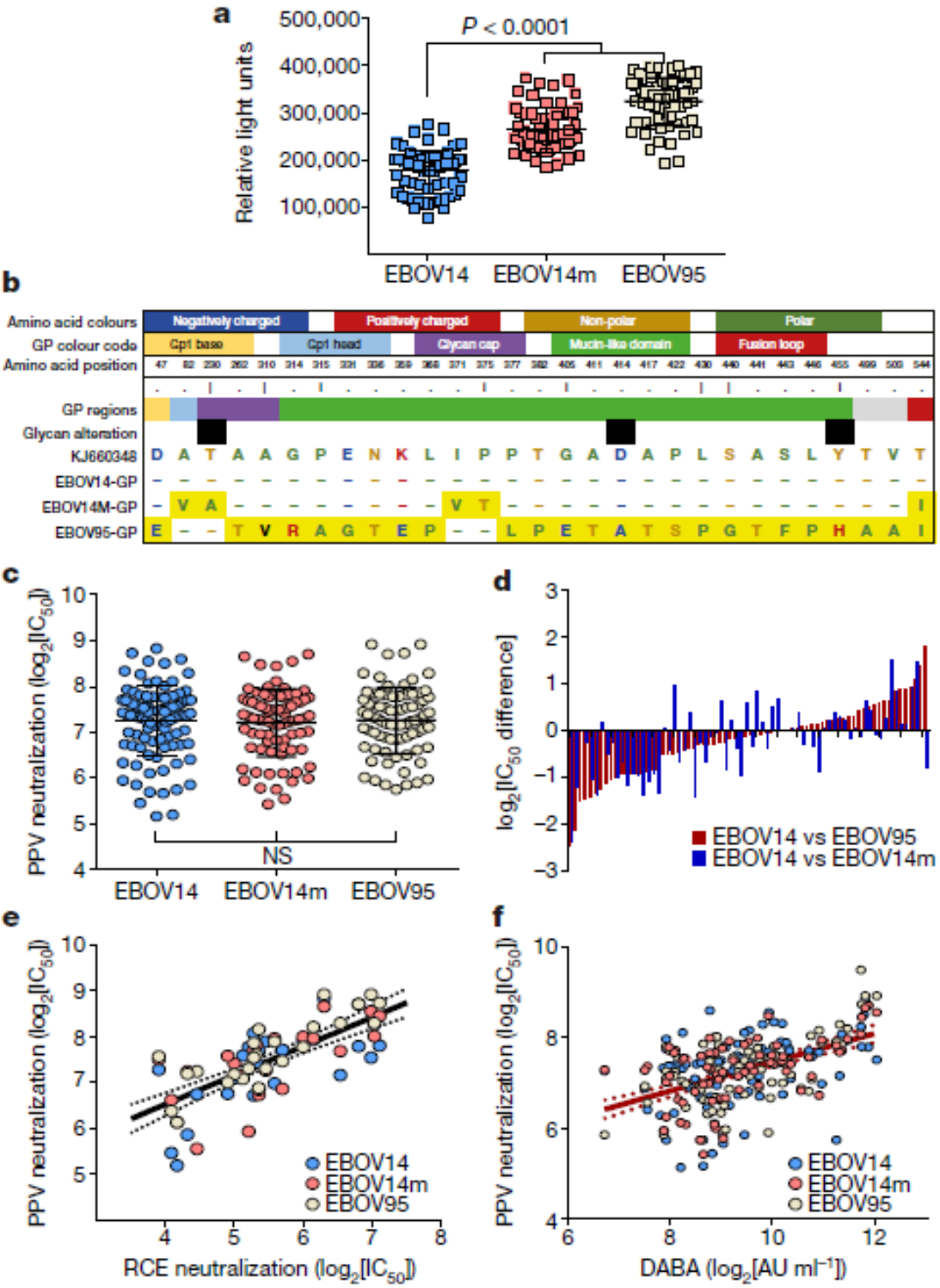
a
P < 0.0001
Relative light units
500,000
400,000
300,000
200,000
100,000
EBOV14
EBOV14m
EBOV95
b
Amino acid colours
Negatively charged
Positively charged
Non-polar
Polar
GP colour code
Cpl base
Cpl head
Glycan cap
Mucin-like domain
Fusion loop
Amino acid position
GP regions
Glycan alteration
KJ660348
EBOV14-GP
EBOV14M-GP
EBOV95-GP
c
PPV neutralization (log2[IC50])
NS
EBOV14
EBOV14m
EBOV95
d
log2[IC50 difference]
EBOV14 vs EBOV95
EBOV14 vs EBOV14m
e
PPV neutralization (log2[IC50])
RCE neutralization (log2[IC50])
EBOV14
EBOV14m
EBOV95
f
PPV neutralization (log2[IC50])
DABA (log2[AU ml−1])
EBOV14
EBOV14m
EBOV95

879

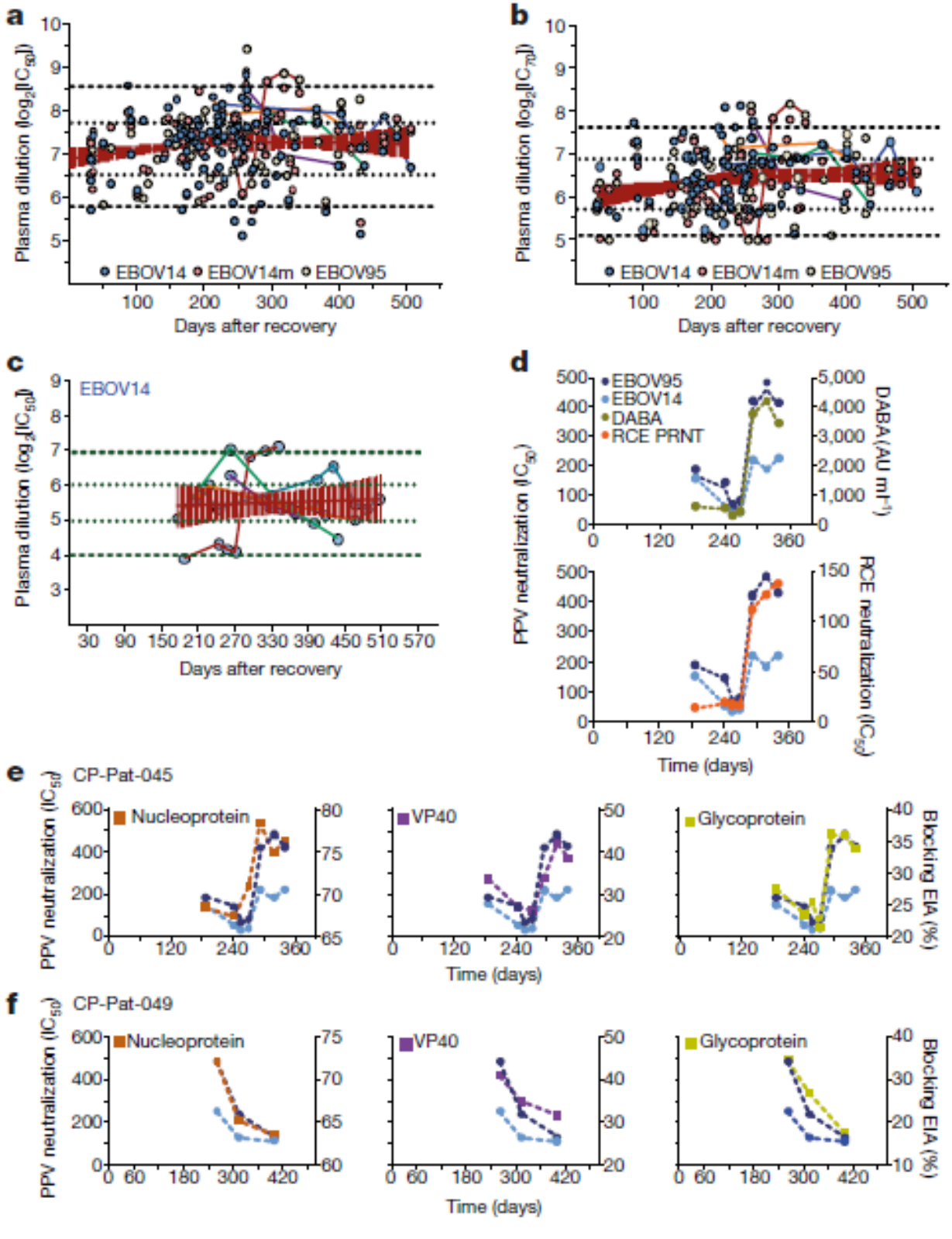
a
Plasma dilution (log2[IC50])
EBOV14 EBOV14m EBOV95
Days after recovery
b
Plasma dilution (log2[IC70])
EBOV14 EBOV14m EBOV95
Days after recovery
c
EBOV14
Plasma dilution (log2[IC50])
Days after recovery
d
EBOV95
EBOV14
DABA
RCE PRNT
PPV neutralization (IC50)
DABA (AU ml-1)
RCE neutralization (IC50)
Time (days)
e
CP-Pat-045
Nucleoprotein
VP40
Glycoprotein
PPV neutralization (IC50)
Blocking EIA (%)
Time (days)
f
CP-Pat-049
Nucleoprotein
VP40
Glycoprotein
PPV neutralization (IC50)
Blocking EIA (%)
Time (days)

880

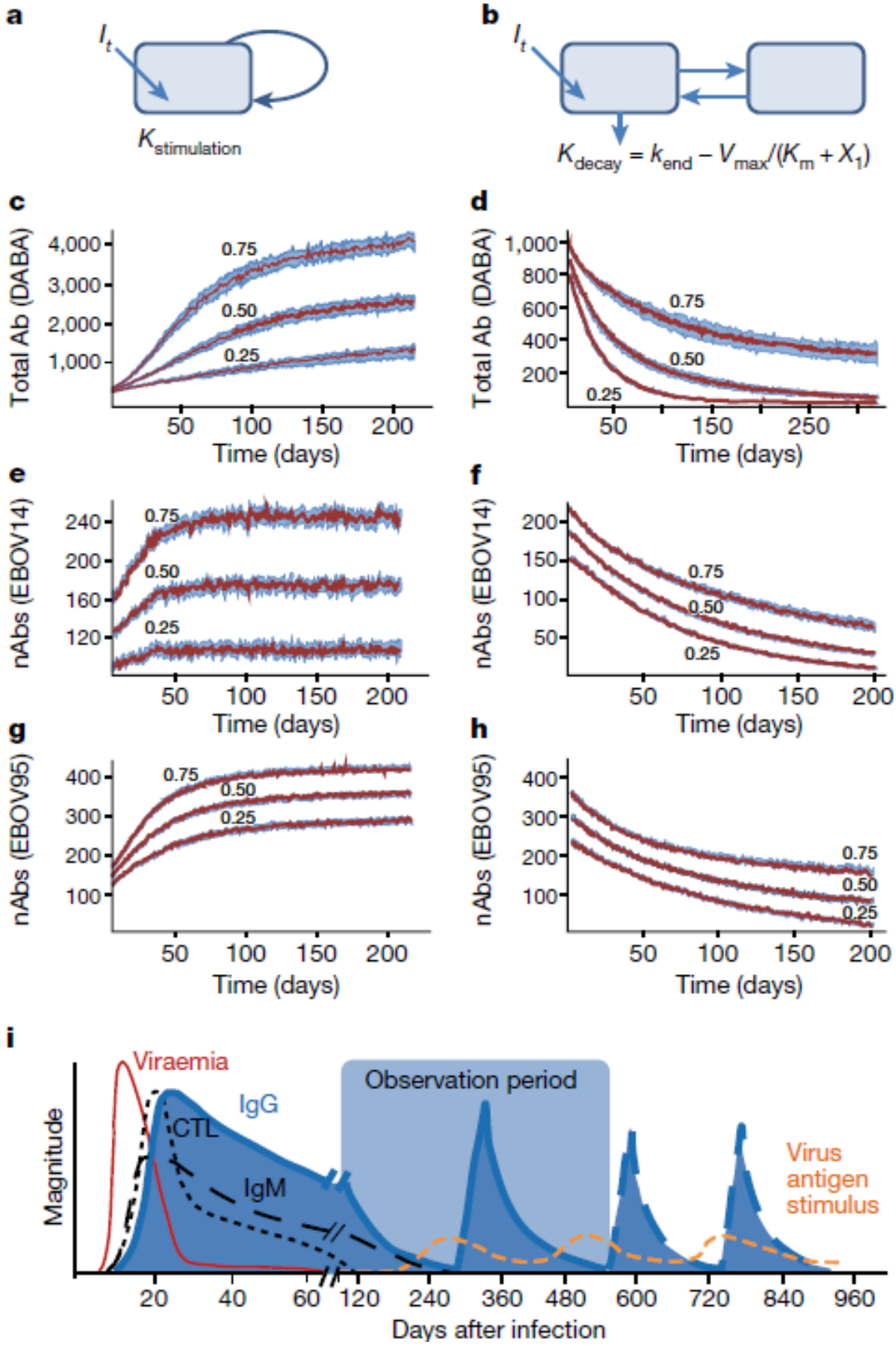
a
I_t
$K_{stimulation}$
b
I_t
$K_{decay} = k_{end} - V_{max}/(K_m + X_1)$
c
Total Ab (DABA)
4,000
3,000
2,000
1,000
0.75
0.50
0.25
50
100
150
200
Time (days)
d
Total Ab (DABA)
1,000
800
600
400
200
0.75
0.50
0.25
50
150
250
Time (days)
e
nAbs (EBOV14)
240
200
160
120
0.75
0.50
0.25
50
100
150
200
Time (days)
f
nAbs (EBOV14)
200
150
100
50
0.75
0.50
0.25
50
100
150
200
Time (days)
g
nAbs (EBOV95)
400
300
200
100
0.75
0.50
0.25
50
100
150
200
Time (days)
h
nAbs (EBOV95)
400
300
200
100
0.75
0.50
0.25
50
100
150
200
Time (days)
i
Viraemia
IgG
CTL
IgM
Observation period
Virus antigen stimulus
Magnitude
20
40
60
120
240
360
480
600
720
840
960
Days after infection

881

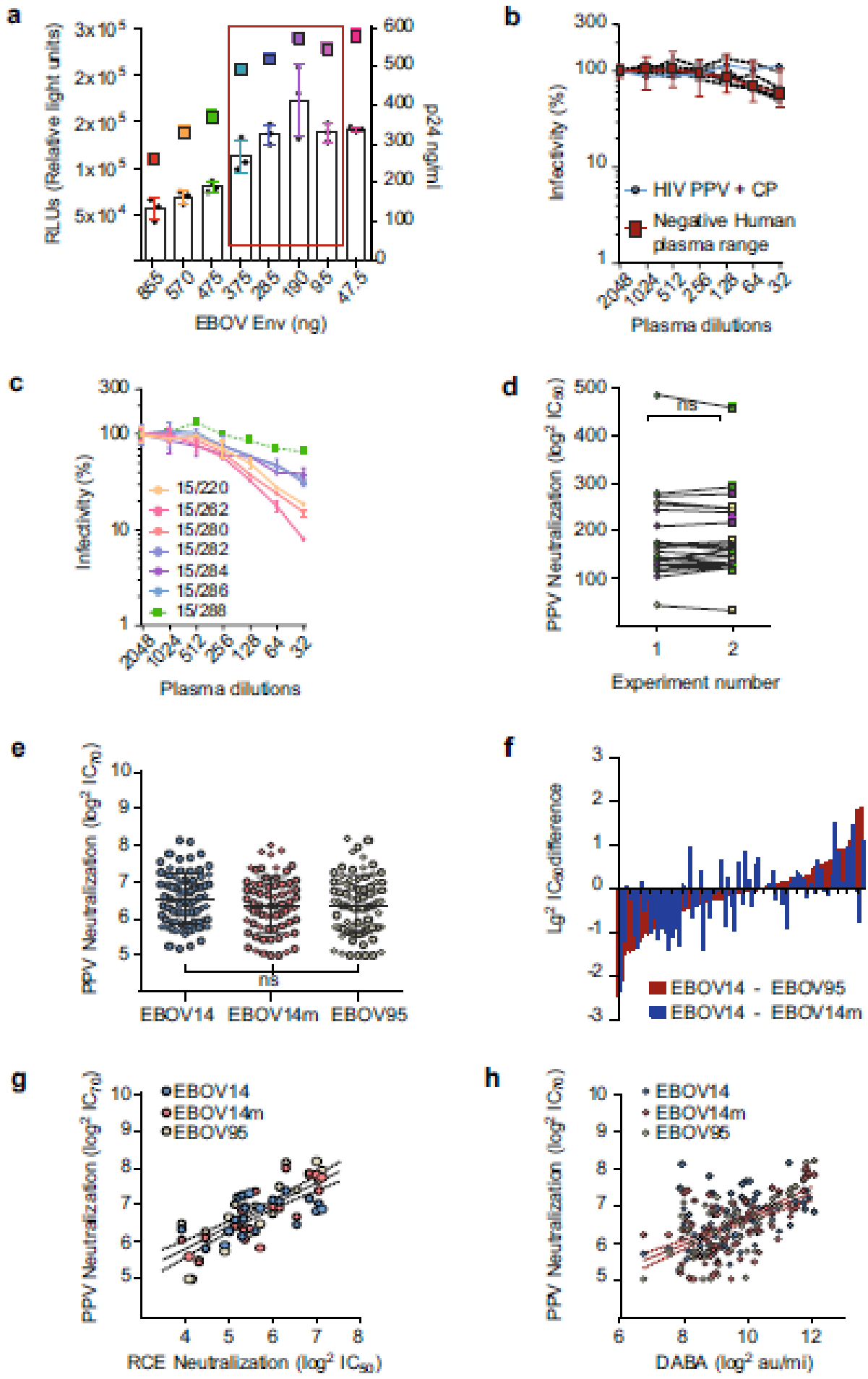
a
RLUs (Relative light units)
3x10^5
2x10^5
2x10^5
1x10^5
5x10^4
600
500
400
300
200
100
0
p24 ng/ml
665
570
475
375
285
190
95
47.5
EBOV Env (ng)
b
Infectivity (%)
300
100
10
1
HIV PPV + CP
Negative Human plasma range
2048
1024
512
256
128
64
32
Plasma dilutions
c
Infectivity (%)
300
100
10
1
15/220
15/262
15/280
15/282
15/284
15/286
15/288
2048
1024
512
256
128
64
32
Plasma dilutions
d
PPV Neutralization (log2 IC50)
500
400
300
200
100
ns
1
2
Experiment number
e
PPV Neutralization (log2 IC70)
10
9
8
7
6
5
ns
EBOV14
EBOV14m
EBOV95
f
Lg2 IC50difference
3
2
1
0
-1
-2
-3
EBOV14 - EBOV95
EBOV14 - EBOV14m
g
PPV Neutralization (log2 IC70)
10
9
8
7
6
5
EBOV14
EBOV14m
EBOV95
4
5
6
7
8
RCE Neutralization (log2 IC50)
h
PPV Neutralization (log2 IC70)
10
9
8
7
6
5
EBOV14
EBOV14m
EBOV95
6
8
10
12
DABA (log2 au/ml)

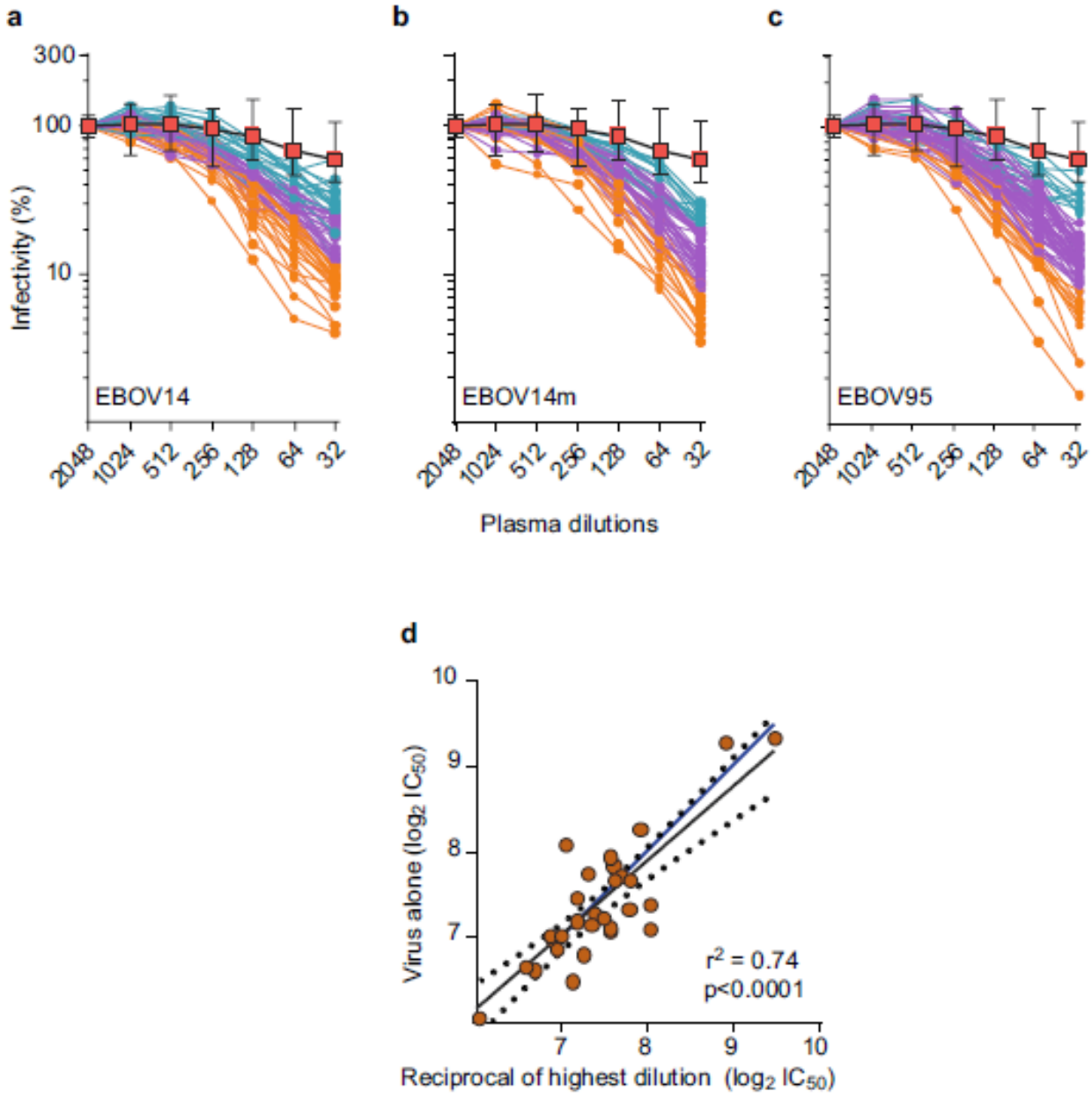
a
b
c
300
100
10
Infectivity (%)
EBOV14
EBOV14m
EBOV95
2048
1024
512
256
128
64
32
Plasma dilutions
d
10
9
8
7
Virus alone (log2 IC50)
r2 = 0.74
p<0.0001
7
8
9
10
Reciprocal of highest dilution (log2 IC50)

883

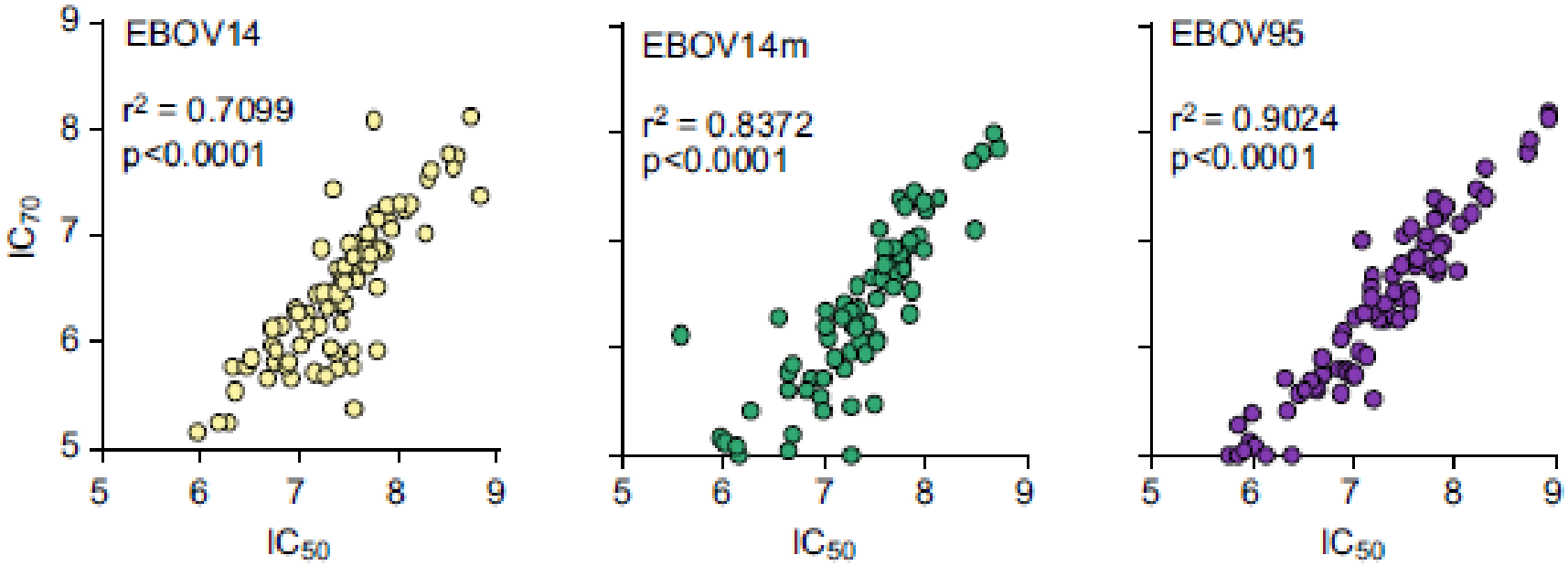
EBOV14
r^2 = 0.7099
p<0.0001
EBOV14m
r^2 = 0.8372
p<0.0001
EBOV95
r^2 = 0.9024
p<0.0001
IC_{70}
IC_{50}
IC_{50}
IC_{50}
5
6
7
8
9

884

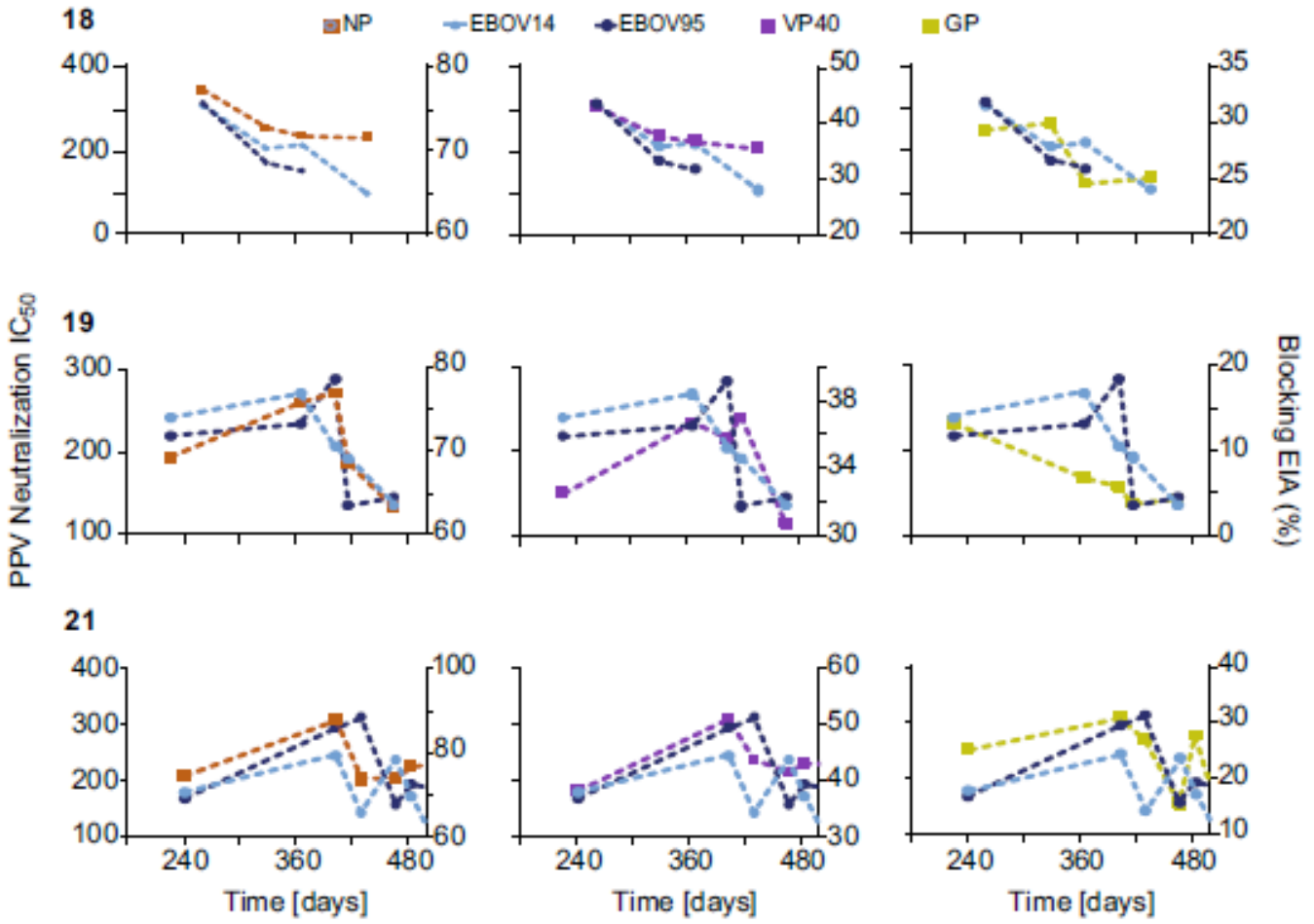

Extended Data Fig. 4 | Longitudinal post convalescence nAb variation in the plasma of individuals 18, 19 and 21 demonstrated by pseudotyped virus particle neutralization. Anti-EBOV14-GP (light blue) and anti-EBOV95-GP (dark blue) nAb titres were overlaid with the blocking EIAs carried out for the detection of antibody against the nucleoprotein [NP] (brown squares), the viral matrix protein 40 [VP40] (purple squares) and the glycoprotein [GP] (green squares).

885

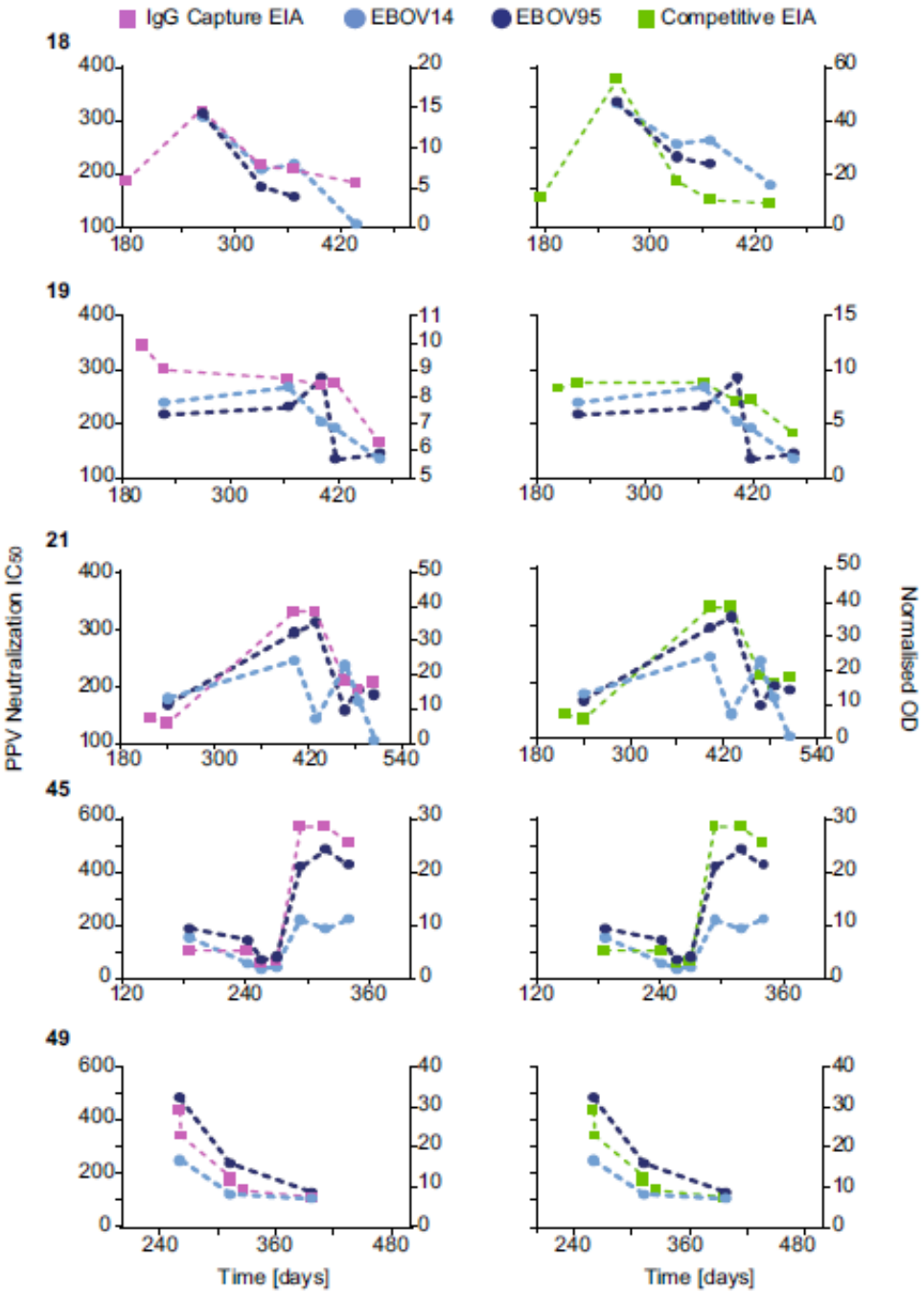
IgG Capture EIA
EBOV14
EBOV95
Competitive EIA
18
19
21
45
49
PPV Neutralization IC50
Normalised OD
Time [days]
Time [days]

886

887

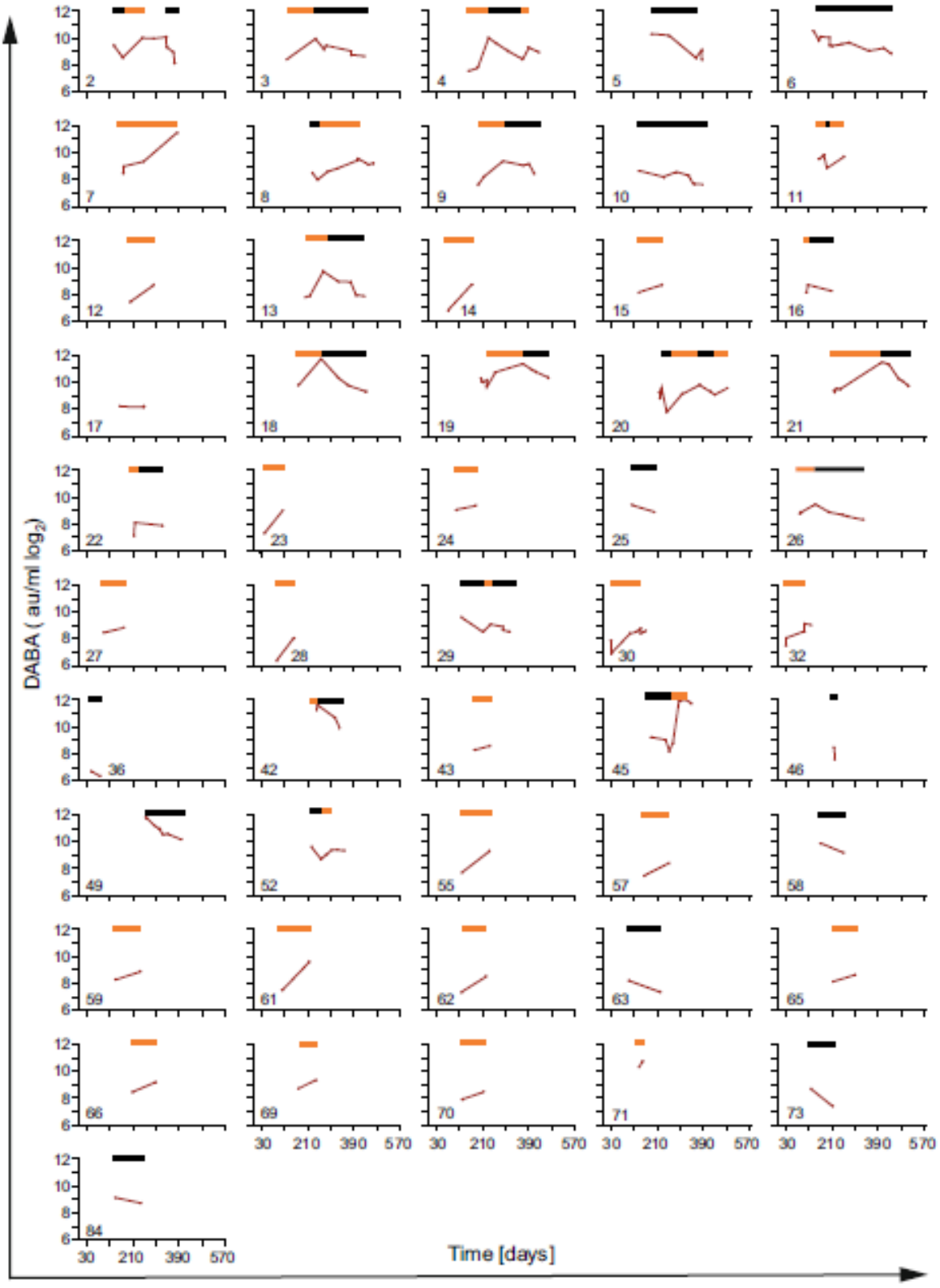
DABA (au/ml log2)
Time [days]
2
3
4
5
6
7
8
9
10
11
12
13
14
15
16
17
18
19
20
21
22
23
24
25
26
27
28
29
30
32
36
42
43
45
46
49
52
55
57
58
59
61
62
63
65
66
69
70
71
73
84
30
210
390
570

8

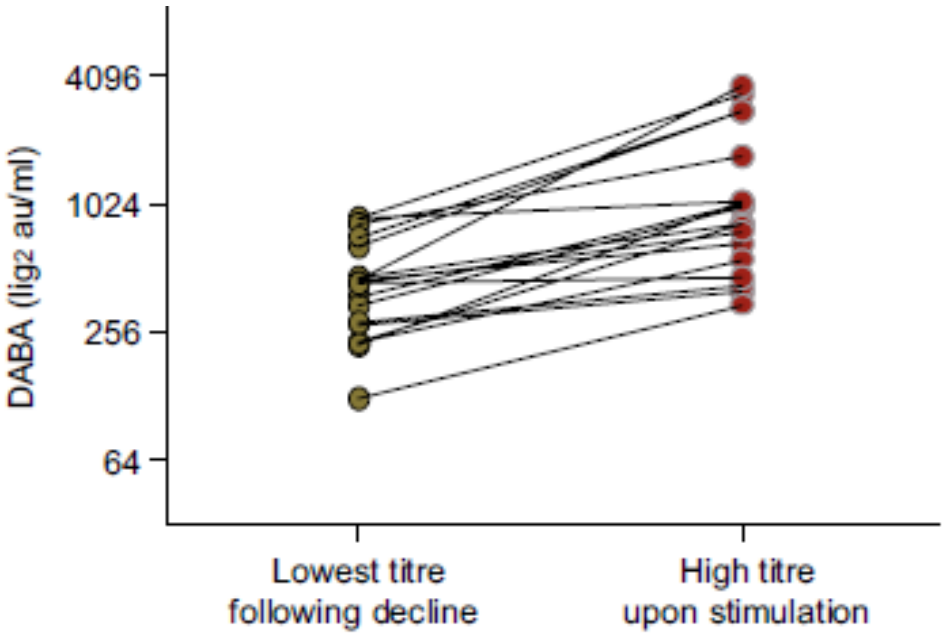
4096
1024
256
64
DABA (lig2 au/ml)
Lowest titre
following decline
High titre
upon stimulation

889

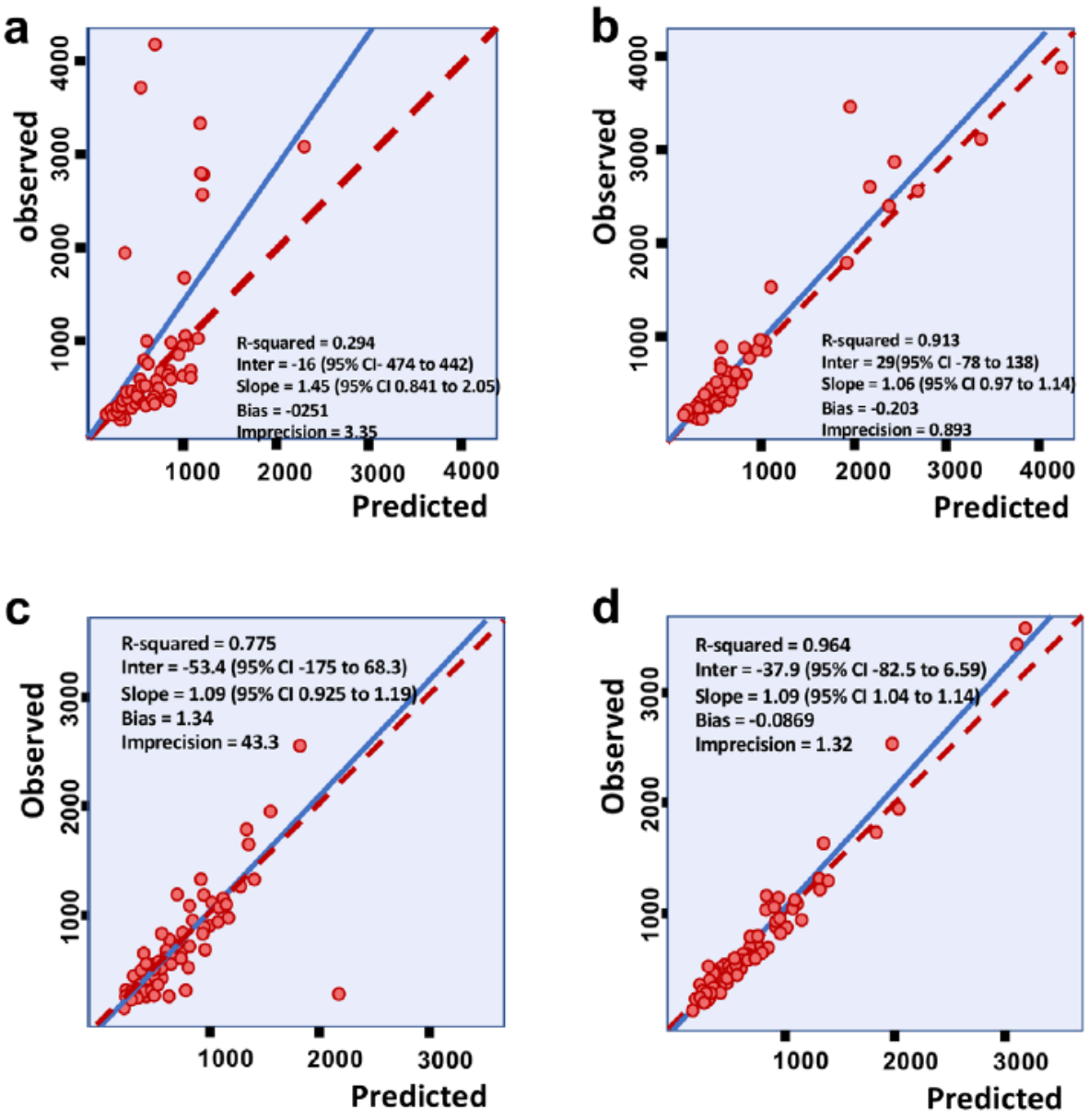
a
observed
1000
2000
3000
4000
R-squared = 0.294
Inter = -16 (95% CI- 474 to 442)
Slope = 1.45 (95% CI 0.841 to 2.05)
Bias = -0251
Imprecision = 3.35
1000
2000
3000
4000
Predicted
b
Observed
1000
2000
3000
4000
R-squared = 0.913
Inter = 29(95% CI -78 to 138)
Slope = 1.06 (95% CI 0.97 to 1.14)
Bias = -0.203
Imprecision = 0.893
1000
2000
3000
4000
Predicted
c
Observed
1000
2000
3000
R-squared = 0.775
Inter = -53.4 (95% CI -175 to 68.3)
Slope = 1.09 (95% CI 0.925 to 1.19)
Bias = 1.34
Imprecision = 43.3
1000
2000
3000
Predicted
d
Observed
1000
2000
3000
R-squared = 0.964
Inter = -37.9 (95% CI -82.5 to 6.59)
Slope = 1.09 (95% CI 1.04 to 1.14)
Bias = -0.0869
Imprecision = 1.32
1000
2000
3000
Predicted

890

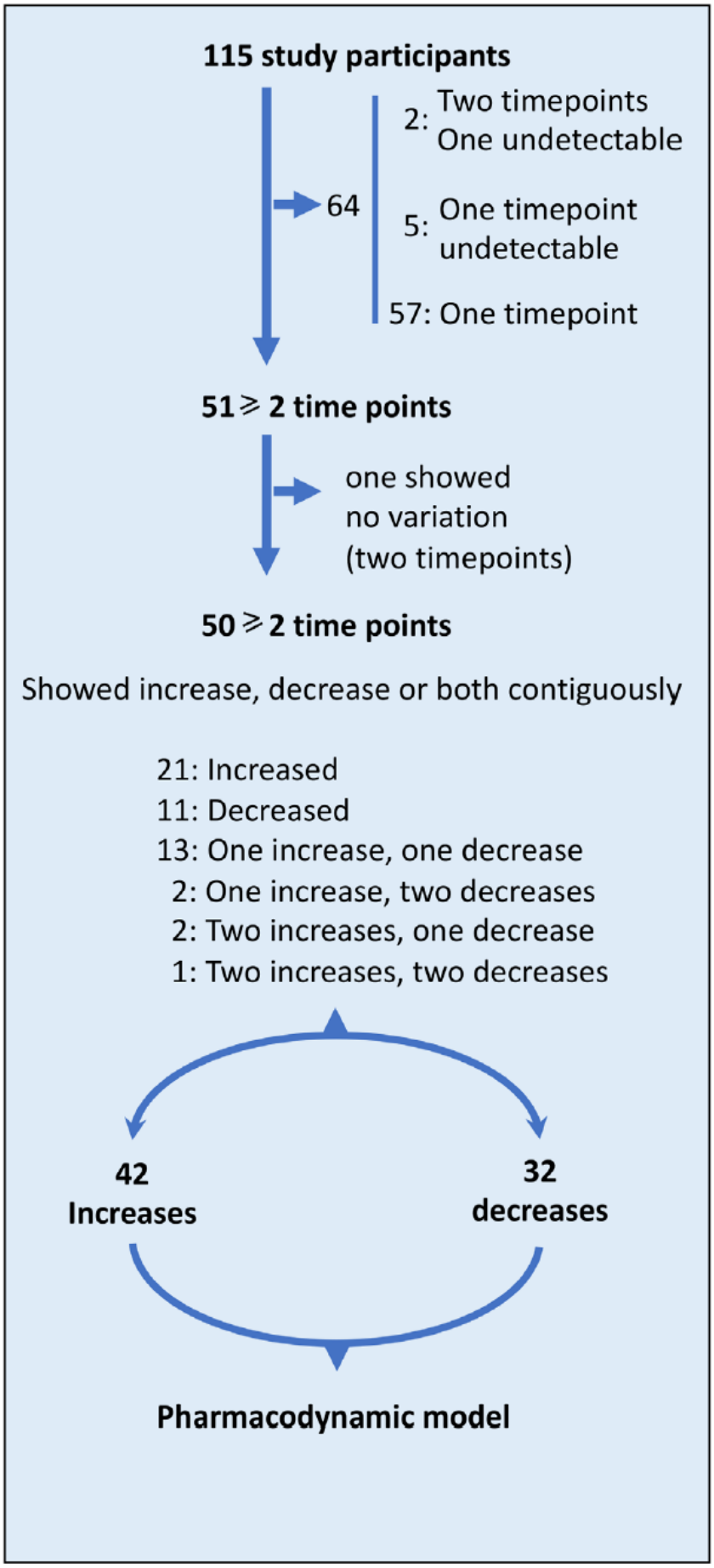
115 study participants
64
2: Two timepoints
One undetectable
5: One timepoint
undetectable
57: One timepoint
51 ⩾ 2 time points
one showed
no variation
(two timepoints)
50 ⩾ 2 time points
Showed increase, decrease or both contiguously
21: Increased
11: Decreased
13: One increase, one decrease
2: One increase, two decreases
2: Two increases, one decrease
1: Two increases, two decreases
42
Increases
32
decreases
Pharmacodynamic model

891

892

Ebola virus antibody decay-stimulation in a high proportion of survivors

Contents	
Supplementary Table 1a:	Ebola survivor study participants
Supplementary Table 1b:	Neutralising titres against PPV-EBOV14
Supplementary Table 1c:	Neutralising titres against PPV-EBOV14m
Supplementary Table 1d:	Neutralising titres against PPV-EBOV95
Supplementary Table 1e:	Neutralising titres against RCF-EBOV14
Supplementary Table 1f:	DABA total antibody titres
Supplementary Table 2:	Amino-acid alignment of the Ebola glycoprotein
Supplementary Table 3a:	Rationale for selection of DABA antibody stimulation structural models
Supplementary Table 3b:	Rationale for selection of DABA antibody decay structural models
Supplementary Table 3c:	Credibility intervals for selected DABA antibody stimulation and decay structural models.
Supplementary Table 4:	Fitted population parameters for IgG restimulation and decay compartmental models.

893

894

Supplementary Table 1a: Ebola survivor study participants. The last positive PCR test was considered as the day 0 post-cure if this information was not available the day 0 was the day of discharge from the ETU.

Donor ID	Sex	Age	BMI	Discharge from ETU	Last antigen positive test	Conscious on arrival at ETU	Conscious throughout	Comparative severity
EBOV-CP-Pat-001	Male	32	24.7	18/10/2014		n	n	n
EBOV-CP-Pat-002	Male	52	21.6		29/11/2014	n	n	n
EBOV-CP-Pat-003	Male	36	21.5		06/12/2014	n	n	n
EBOV-CP-Pat-004	Male	30	19.3		10/11/2014	n	n	n
EBOV-CP-Pat-005	Male	30	22.3		20/11/2014	n	n	n
EBOV-CP-Pat-006	Female	29	27.7	13/12/2014		n	n	n
EBOV-CP-Pat-007	Male	22	24.6		22/11/2014	n	n	n
EBOV-CP-Pat-008	Male	27	21.8	13/09/2014		n	n	n
EBOV-CP-Pat-009	Male	26	19.2	19/10/2014		n	n	n
EBOV-CP-Pat-010	Male	27	24.1	20/12/2014		n	n	n
EBOV-CP-Pat-011	Male	27	20.3	29/11/2014		n	n	n
EBOV-CP-Pat-012	Male	27	26.1	18/10/2014		n	n	n
EBOV-CP-Pat-013	Female	34	26.6	08/11/2014		n	n	n
EBOV-CP-Pat-014	Male	37	22.7	15/02/2015		n	n	n
EBOV-CP-Pat-015	Male	26	21.9	17/12/2014		n	n	n
EBOV-CP-Pat-016	Male	22	24.5	08/01/2015		n	n	n
EBOV-CP-Pat-017	Male	25	24.6	28/11/2014		n	n	n
EBOV-CP-Pat-018	Female	42	25.1		17/11/2014	n	n	n
EBOV-CP-Pat-019	Female	40	22.2	19/10/2014		n	n	n
EBOV-CP-Pat-020	Female	38	20.2	04/10/2014		n	n	n
EBOV-CP-Pat-021	Male	21	22.3	04/10/2014		n	n	n
EBOV-CP-Pat-022	Male	21	20.9	04/10/2014		n	n	n
EBOV-CP-Pat-023	Male	25	23.8	10/04/2015		n	n	n
EBOV-CP-Pat-024	Female	24	25.3	26/11/2015		n	n	n
EBOV-CP-Pat-025	Male	19	20.2		05/02/2015	n	n	n
EBOV-CP-Pat-026	Female	26	25.2		15/03/2015	n	n	n
EBOV-CP-Pat-027	Female	25	28.3	02/03/2015		n	n	n
EBOV-CP-Pat-028	Male	35	29.1	09/03/2015		n	n	n
EBOV-CP-Pat-029	Male	26	26.3	30/01/2015		1	1	1
EBOV-CP-Pat-030	Male	35	19.1	18/07/2015		n	n	n
EBOV-CP-Pat-031	Female	25	23.5		22/07/2015	1	n	3
EBOV-CP-Pat-032	Female	22	23.2	20/07/2015		1	1	2
EBOV-CP-Pat-033	Female	22	32	23/07/2015		1	1	2
EBOV-CP-Pat-034	Female	22	24.3	16/05/2015		1	1	1
EBOV-CP-Pat-035	Female	21	21.5	25/01/2015		1	1	2

EBOV-CP-Pat-036	Male	28	23.2	23/07/2015		1	1	1
EBOV-CP-Pat-037	Male	18	23.1	15/01/2015		n	n	3
EBOV-CP-Pat-038	Male	33	20.8	10/07/2015		1	1	1
EBOV-CP-Pat-039	Female	21	20.8	10/06/2015		n	n	3
EBOV-CP-Pat-040	Male	28	21.8	30/03/2015		1	1	1
EBOV-CP-Pat-041	Male	20	22.9	18/03/2015		1	n	2
EBOV-CP-Pat-042	Female	27	25.4	10/01/2015		1	n	2
EBOV-CP-Pat-043	Male	38	21.5	14/03/2015		1	1	1
EBOV-CP-Pat-044	Male	19	26.7	11/06/2015		1	n	3
EBOV-CP-Pat-045	Female	18	21.3	18/03/2015		n	n	3
EBOV-CP-Pat-046	Male	42	23.1	20/02/2015		1	1	2
EBOV-CP-Pat-047	Male	23	20.1	24/03/2015		1	1	2
EBOV-CP-Pat-048	Male	23	24.2	20/03/2015		1	1	1
EBOV-CP-Pat-049	Male	22	20.7	15/01/2015		n	1	2
EBOV-CP-Pat-050	Male	18	20.5	08/04/2015		1	1	2
EBOV-CP-Pat-051	Male	22	22.6	25/03/2015		1	1	1
EBOV-CP-Pat-052	Male	28	25.1	20/02/2015		1	1	2
EBOV-CP-Pat-053	Male	30	23.8	12/01/2015		n	n	n
EBOV-CP-Pat-054	Male	32	18.9	30/03/2015		n	n	n
EBOV-CP-Pat-055	Male	21	25.7	13/12/2014		n	n	n
EBOV-CP-Pat-056	Male	39	25.3	30/01/2015		n	n	n
EBOV-CP-Pat-057	Male	27	30.1	22/11/2014		n	n	n
EBOV-CP-Pat-058	Female	27	26.4	21/11/2014		n	n	n
EBOV-CP-Pat-059	Male	29	23.4	08/12/2014		n	n	n
EBOV-CP-Pat-060	Male	43	24.8	17/03/2015		n	n	n
EBOV-CP-Pat-061	Male	42	30.3	08/01/2015		n	n	n
EBOV-CP-Pat-062	Male	39	23.9	24/12/2014		n	n	n
EBOV-CP-Pat-063	Male	37	23.8	20/01/2015		n	n	n
EBOV-CP-Pat-064	Male	25	19.5	15/02/2015		n	n	n
EBOV-CP-Pat-065	Male	34	21	03/10/2014		n	n	n
EBOV-CP-Pat-066	Male	40	24.1	09/10/2014		n	n	n
EBOV-CP-Pat-067	Male	20	23	06/12/2014		n	n	n
EBOV-CP-Pat-068	Male	51	21.4	10/04/2015		n	n	n
EBOV-CP-Pat-069	Male	22	19.6	06/12/2014		n	n	n
EBOV-CP-Pat-070	Male	25	21.5	26/01/2015		n	n	n
EBOV-CP-Pat-071	Male	27	24.5	20/01/2015		n	n	n
EBOV-CP-Pat-072	Male	40	21.7	20/07/2015		n	n	n
EBOV-CP-Pat-073	Male	36	23.4	28/01/2015		n	n	n
EBOV-CP-Pat-074	Male	24	28.4	16/01/2015		n	n	n
EBOV-CP-Pat-075	Male	23	27.3	06/10/2014		n	n	n
EBOV-CP-Pat-076	Male	19	22.3	30/04/2015		n	n	n
EBOV-CP-Pat-077	Male	33	20.1	18/01/2015		n	n	n
EBOV-CP-Pat-078	Female	31	18.6	03/01/2015		n	n	n
EBOV-CP-Pat-079	Male	25	21.3	07/01/2015		n	n	n

896

EBOV-CP-Pat-080	Female	27	21.8	01/01/2015		n	n	n
EBOV-CP-Pat-081	Female	33	18.4	02/04/2015		n	n	n
EBOV-CP-Pat-082	Male	20	19.6	15/01/2015		n	n	n
EBOV-CP-Pat-083	Male	22	20	12/01/2015		n	n	n
EBOV-CP-Pat-084	Male	33	21.6	05/05/2015		n	n	n
EBOV-CP-Pat-085	Male	25	25.4	19/12/2014		n	n	n
EBOV-CP-Pat-086	Female	43	18.4	10/12/2014		n	n	n
EBOV-CP-Pat-087	Male	41	22.1	06/12/2014		n	n	n
EBOV-CP-Pat-088	Female	22	21.2	22/12/2014		n	n	n
EBOV-CP-Pat-089	Male	35	20.8	08/08/2015		n	n	n
EBOV-CP-Pat-090	Male	24	21	14/01/2015		n	n	n
EBOV-CP-Pat-091	Male	20	19.4	06/02/2015		n	n	n
EBOV-CP-Pat-092	Male	38	20.3	10/12/2014		n	n	n
EBOV-CP-Pat-093	Male	22	22.6	25/02/2015		n	n	n
EBOV-CP-Pat-094	Male	30	25.7	08/02/2015		n	n	n
EBOV-CP-Pat-095	Female	25	29.7	20/01/2015		n	n	n
EBOV-CP-Pat-096	Female	33	25.7	20/01/2015		n	n	n
EBOV-CP-Pat-097	Female	40	30.8	18/01/2015		n	n	n
EBOV-CP-Pat-098	Female	31	22.9	18/01/2015		n	n	n
EBOV-CP-Pat-099	Male	35	22.9	09/03/2015		n	n	n
EBOV-CP-Pat-100	Male	21	21.8	25/01/2015		n	n	n
EBOV-CP-Pat-101	Female	24	25	25/03/2015		n	n	n
EBOV-CP-Pat-102	Female	33	30.8	18/01/2015		n	n	n
EBOV-CP-Pat-103	Male	35	23.6	24/02/2015		n	n	n
EBOV-CP-Pat-104	Female	19	22.8	02/01/2015		n	n	n
EBOV-CP-Pat-105	Male	40	21.7	02/02/2015		n	n	n
EBOV-CP-Pat-106	Male	24	22.9	28/03/2015		n	n	n
EBOV-CP-Pat-107	Male	35	23.1	22/03/2015		n	n	n
EBOV-CP-Pat-108	Male	36	22.2	22/03/2015		n	n	n
EBOV-CP-Pat-109	Female	32	30.1	22/03/2015		n	n	n
EBOV-CP-Pat-110	Male	26	30	02/03/2015		n	n	n
EBOV-CP-Pat-111	Male	25	21.5	23/02/2015		n	n	n
EBOV-CP-Pat-112	Female	29	24.8	16/01/2015		n	n	n
EBOV-CP-Pat-113	Female	35	26.7	24/01/2015		n	n	n
EBOV-CP-Pat-114	Male	24	25.4	14/04/2015		n	n	n
EBOV-CP-Pat-115	Female	21	18.3	16/04/2015		n	n	n

1=Yes	1=mild
0=No	2=mod
n=no data	3=Sev
	n=no data

897

Supplementary Table 1b: Neutralising titres against Pseudo-typed virus PPV-EBOV14

Donor ID	DAYS FROM CONVALESCENCE	PPV EBOV14 IC50 inhibiting Dilution	Donor ID	DAYS FROM CONVALESCENCE	PPV EBOV14 IC50 inhibiting Dilution
EBOV-CP-Pat-001	333	147	EBOV-CP-Pat-021	484	173
EBOV-CP-Pat-002	172	106	EBOV-CP-Pat-021	505	105
EBOV-CP-Pat-002	248	198	EBOV-CP-Pat-022	325	62
EBOV-CP-Pat-002	290	186	EBOV-CP-Pat-024	108	220
EBOV-CP-Pat-003	241	189	EBOV-CP-Pat-025	200	124
EBOV-CP-Pat-003	283	58	EBOV-CP-Pat-026	85	388
EBOV-CP-Pat-003	380	51	EBOV-CP-Pat-026	89	258
EBOV-CP-Pat-003	431	35.9	EBOV-CP-Pat-026	145	277
EBOV-CP-Pat-004	191	78	EBOV-CP-Pat-026	199	102
EBOV-CP-Pat-005	188	220	EBOV-CP-Pat-026	271	102
EBOV-CP-Pat-005	256	318	EBOV-CP-Pat-027	173	69
EBOV-CP-Pat-006	158	314	EBOV-CP-Pat-028	156	166
EBOV-CP-Pat-006	164	196	EBOV-CP-Pat-030	31	54
EBOV-CP-Pat-007	172	136	EBOV-CP-Pat-030	145	154
EBOV-CP-Pat-007	173	181	EBOV-CP-Pat-030	166	54
EBOV-CP-Pat-007	251	164	EBOV-CP-Pat-032	31	85
EBOV-CP-Pat-008	228	171	EBOV-CP-Pat-033	32	118
EBOV-CP-Pat-008	249	166	EBOV-CP-Pat-034	100	72
EBOV-CP-Pat-010	138	120	EBOV-CP-Pat-035	217	277
EBOV-CP-Pat-011	257	142	EBOV-CP-Pat-036	82	153
EBOV-CP-Pat-012	290	80	EBOV-CP-Pat-037	240	376
EBOV-CP-Pat-013	216	161	EBOV-CP-Pat-038	65	81
EBOV-CP-Pat-014	169	186	EBOV-CP-Pat-039	95	225
EBOV-CP-Pat-015	229	88	EBOV-CP-Pat-040	168	175
EBOV-CP-Pat-016	208	186	EBOV-CP-Pat-041	179	166
EBOV-CP-Pat-017	252	160	EBOV-CP-Pat-042	244	44
EBOV-CP-Pat-018	262	302	EBOV-CP-Pat-043	179	171
EBOV-CP-Pat-018	330	209	EBOV-CP-Pat-045	186	154
EBOV-CP-Pat-018	368	218	EBOV-CP-Pat-045	242	58.3
EBOV-CP-Pat-018	437	107	EBOV-CP-Pat-045	256	35.2
EBOV-CP-Pat-019	211	324	EBOV-CP-Pat-045	270	43.7
EBOV-CP-Pat-019	226	240	EBOV-CP-Pat-045	293	221
EBOV-CP-Pat-019	259	192	EBOV-CP-Pat-045	318	182
EBOV-CP-Pat-019	365	269	EBOV-CP-Pat-045	340	223
EBOV-CP-Pat-019	402	205	EBOV-CP-Pat-046	220	215
EBOV-CP-Pat-019	417	192	EBOV-CP-Pat-047	193	148
EBOV-CP-Pat-019	465	136	EBOV-CP-Pat-048	197	177
EBOV-CP-Pat-020	218	159	EBOV-CP-Pat-049	261	458
EBOV-CP-Pat-020	219	196	EBOV-CP-Pat-049	262	364
EBOV-CP-Pat-020	220	105	EBOV-CP-Pat-049	292	250
EBOV-CP-Pat-020	226	132	EBOV-CP-Pat-049	313	126
EBOV-CP-Pat-021	218	188	EBOV-CP-Pat-049	398	108
EBOV-CP-Pat-021	219	232	EBOV-CP-Pat-050	180	175
EBOV-CP-Pat-021	226	287	EBOV-CP-Pat-051	193	207
EBOV-CP-Pat-021	403	245	EBOV-CP-Pat-102	277	209
EBOV-CP-Pat-021	430	143			
EBOV-CP-Pat-021	467	237			

898

Supplementary Table 1c: Neutralising titres against Pseudo-typed virus PPV-EBOV14m

Donor ID	DAYS FROM CONVALESCENCE	PPV EBOV14m IC50 inhibiting Dilution	Donor ID	DAYS FROM CONVALESCENCE	PPV EBOV14m IC50 inhibiting Dilution
EBOV-CP-Pat-001	333	99	EBOV-CP-Pat-039	95	218
EBOV-CP-Pat-002	248	170	EBOV-CP-Pat-040	168	194
EBOV-CP-Pat-002	290	196	EBOV-CP-Pat-041	179	221
EBOV-CP-Pat-003	241	175	EBOV-CP-Pat-042	244	227
EBOV-CP-Pat-003	283	151	EBOV-CP-Pat-043	179	185
EBOV-CP-Pat-003	380	55	EBOV-CP-Pat-045	186	181
EBOV-CP-Pat-003	431	43	EBOV-CP-Pat-045	242	151
EBOV-CP-Pat-005	256	178	EBOV-CP-Pat-045	256	70
EBOV-CP-Pat-007	172	112	EBOV-CP-Pat-045	270	98
EBOV-CP-Pat-007	251	115	EBOV-CP-Pat-045	293	418
EBOV-CP-Pat-011	257	124	EBOV-CP-Pat-045	318	375
EBOV-CP-Pat-012	290	127	EBOV-CP-Pat-045	340	349
EBOV-CP-Pat-014	169	159	EBOV-CP-Pat-046	220	76
EBOV-CP-Pat-015	229	163	EBOV-CP-Pat-047	193	143
EBOV-CP-Pat-016	208	68	EBOV-CP-Pat-048	197	135
EBOV-CP-Pat-017	252	181	EBOV-CP-Pat-049	261	403
EBOV-CP-Pat-018	262	271	EBOV-CP-Pat-049	313	248
EBOV-CP-Pat-018	437	142	EBOV-CP-Pat-049	326	114
EBOV-CP-Pat-019	226	255	EBOV-CP-Pat-049	398	191
EBOV-CP-Pat-019	365	209	EBOV-CP-Pat-050	180	168
EBOV-CP-Pat-019	402	106	EBOV-CP-Pat-051	193	357
EBOV-CP-Pat-019	417	142	EBOV-CP-Pat-060	141	130
EBOV-CP-Pat-019	465	171	EBOV-CP-Pat-102	277	190
EBOV-CP-Pat-021	403	250			
EBOV-CP-Pat-021	430	205			
EBOV-CP-Pat-021	467	153			
EBOV-CP-Pat-021	484	227			
EBOV-CP-Pat-021	505	196			
EBOV-CP-Pat-022	325	62			
EBOV-CP-Pat-023	115	102			
EBOV-CP-Pat-024	108	102			
EBOV-CP-Pat-025	200	146			
EBOV-CP-Pat-026	85	255			
EBOV-CP-Pat-026	89	203			
EBOV-CP-Pat-026	145	230			
EBOV-CP-Pat-026	199	64			
EBOV-CP-Pat-026	271	54			
EBOV-CP-Pat-027	173	68			
EBOV-CP-Pat-028	156	211			
EBOV-CP-Pat-030	166	125			
EBOV-CP-Pat-031	35	99			
EBOV-CP-Pat-032	31	165			
EBOV-CP-Pat-033	32	155			
EBOV-CP-Pat-034	100	69			
EBOV-CP-Pat-035	217	95			
EBOV-CP-Pat-036	82	156			
EBOV-CP-Pat-038	65	203			

899

Supplementary Table 1d: Neutralising titres against Pseudo-typed virus PPV-EBOV95

Donor ID	DAYS FROM CONVALESCENCE	PPV EBOV95 IC50 inhibiting Dilution	Donor ID	DAYS FROM CONVALESCENCE	PPV EBOV95 IC50 inhibiting Dilution
EBOV-CP-Pat-001	333	158	EBOV-CP-Pat-033	32	122
EBOV-CP-Pat-002	248	225	EBOV-CP-Pat-034	100	65
EBOV-CP-Pat-002	290	129	EBOV-CP-Pat-036	82	58
EBOV-CP-Pat-003	241	102	EBOV-CP-Pat-037	240	189
EBOV-CP-Pat-003	283	108	EBOV-CP-Pat-038	65	143
EBOV-CP-Pat-003	380	62	EBOV-CP-Pat-039	95	221
EBOV-CP-Pat-003	431	99	EBOV-CP-Pat-040	168	116
EBOV-CP-Pat-005	256	175	EBOV-CP-Pat-041	179	220
EBOV-CP-Pat-007	172	115	EBOV-CP-Pat-042	244	241
EBOV-CP-Pat-007	251	166	EBOV-CP-Pat-043	238	126
EBOV-CP-Pat-060	141	225	EBOV-CP-Pat-044	95	178
EBOV-CP-Pat-011	257	119	EBOV-CP-Pat-045	186	189
EBOV-CP-Pat-012	290	98	EBOV-CP-Pat-045	242	146
EBOV-CP-Pat-014	169	162	EBOV-CP-Pat-045	256	70
EBOV-CP-Pat-015	229	80	EBOV-CP-Pat-045	270	83
EBOV-CP-Pat-016	208	88	EBOV-CP-Pat-045	293	418
EBOV-CP-Pat-017	252	132	EBOV-CP-Pat-045	318	483
EBOV-CP-Pat-018	262	717	EBOV-CP-Pat-045	340	425
EBOV-CP-Pat-018	330	177	EBOV-CP-Pat-046	220	137
EBOV-CP-Pat-018	368	158	EBOV-CP-Pat-047	193	210
EBOV-CP-Pat-018	437	151	EBOV-CP-Pat-048	197	229
EBOV-CP-Pat-019	226	218	EBOV-CP-Pat-049	261	483
EBOV-CP-Pat-019	259	263	EBOV-CP-Pat-049	313	237
EBOV-CP-Pat-019	365	232	EBOV-CP-Pat-049	326	118
EBOV-CP-Pat-019	402	286	EBOV-CP-Pat-049	398	128
EBOV-CP-Pat-019	417	135	EBOV-CP-Pat-050	180	143
EBOV-CP-Pat-019	465	145	EBOV-CP-Pat-051	193	60
EBOV-CP-Pat-021	403	295	EBOV-CP-Pat-075	322	91
EBOV-CP-Pat-021	430	313	EBOV-CP-Pat-102	277	113
EBOV-CP-Pat-021	467	173			
EBOV-CP-Pat-021	484	194			
EBOV-CP-Pat-021	505	186			
EBOV-CP-Pat-022	325	58			
EBOV-CP-Pat-023	115	81			
EBOV-CP-Pat-024	108	63			
EBOV-CP-Pat-025	200	259			
EBOV-CP-Pat-026	145	181			
EBOV-CP-Pat-026	199	103			
EBOV-CP-Pat-026	271	54			
EBOV-CP-Pat-027	173	197			
EBOV-CP-Pat-028	156	151			
EBOV-CP-Pat-072	34	139			
EBOV-CP-Pat-030	31	153			
EBOV-CP-Pat-030	129	120			
EBOV-CP-Pat-030	166	233			
EBOV-CP-Pat-031	35	187			
EBOV-CP-Pat-032	31	95			

900

Supplementary Table 1e: Neutralising titres against Replication Competent Ebola virus *RCE*-EBOV14

Donor ID	DAYS FROM CONVALESCENCE	RCF EBOV14 IC50 inhibiting Dilution
EBOV-CP-Pat-018	175	33
EBOV-CP-Pat-018	262	131
EBOV-CP-Pat-018	330	52
EBOV-CP-Pat-018	368	37
EBOV-CP-Pat-018	437	22
EBOV-CP-Pat-019	204	47
EBOV-CP-Pat-019	226	64
EBOV-CP-Pat-019	365	39
EBOV-CP-Pat-019	402	41
EBOV-CP-Pat-019	417	35
EBOV-CP-Pat-019	465	32
EBOV-CP-Pat-021	218	59
EBOV-CP-Pat-021	241	40
EBOV-CP-Pat-021	403	71
EBOV-CP-Pat-021	430	93
EBOV-CP-Pat-021	467	44
EBOV-CP-Pat-021	484	40
EBOV-CP-Pat-021	505	49
EBOV-CP-Pat-021	218	59
EBOV-CP-Pat-021	241	40
EBOV-CP-Pat-021	403	71
EBOV-CP-Pat-021	430	93
EBOV-CP-Pat-021	467	44
EBOV-CP-Pat-021	484	40
EBOV-CP-Pat-021	505	49
EBOV-CP-Pat-045	186	15
EBOV-CP-Pat-045	242	20
EBOV-CP-Pat-045	256	18
EBOV-CP-Pat-045	270	17
EBOV-CP-Pat-045	293	112
EBOV-CP-Pat-045	318	127
EBOV-CP-Pat-045	340	138
EBOV-CP-Pat-049	261	79
EBOV-CP-Pat-049	313	48
EBOV-CP-Pat-049	326	41
EBOV-CP-Pat-049	345	40
EBOV-CP-Pat-049	398	30

901

Supplementary Table 1f: Double antigen bridging assay (DABA) antibody titres

Donor ID	DAYS FROM CONVALESCENCE	DABA au/ml	Donor ID	DAYS FROM CONVALESCENCE	DABA au/ml
EBOV-CP-Pat-001	179	nd	EBOV-CP-Pat-008	324	451
EBOV-CP-Pat-001	333	500	EBOV-CP-Pat-008	403	680
EBOV-CP-Pat-002	137	721	EBOV-CP-Pat-008	404	747
EBOV-CP-Pat-002	172	384	EBOV-CP-Pat-008	445	553
EBOV-CP-Pat-002	248	1048	EBOV-CP-Pat-008	465	591
EBOV-CP-Pat-002	290	1019	EBOV-CP-Pat-009	191	198
EBOV-CP-Pat-002	339	1093	EBOV-CP-Pat-009	212	296
EBOV-CP-Pat-002	340	659	EBOV-CP-Pat-009	287	660
EBOV-CP-Pat-002	367	496	EBOV-CP-Pat-009	365	530
EBOV-CP-Pat-002	371	285	EBOV-CP-Pat-009	388	567
EBOV-CP-Pat-003	130	344	EBOV-CP-Pat-009	408	347
EBOV-CP-Pat-003	241	1001	EBOV-CP-Pat-010	138	334
EBOV-CP-Pat-003	274	584	EBOV-CP-Pat-010	236	283
EBOV-CP-Pat-003	283	704	EBOV-CP-Pat-010	284	399
EBOV-CP-Pat-003	380	528	EBOV-CP-Pat-010	332	357
EBOV-CP-Pat-003	380	434	EBOV-CP-Pat-010	353	242
EBOV-CP-Pat-003	431	402	EBOV-CP-Pat-010	383	247
EBOV-CP-Pat-004	156	190	EBOV-CP-Pat-011	160	755
EBOV-CP-Pat-004	191	225	EBOV-CP-Pat-011	179	933
EBOV-CP-Pat-004	233	1061	EBOV-CP-Pat-011	191	474
EBOV-CP-Pat-004	263	800	EBOV-CP-Pat-011	257	853
EBOV-CP-Pat-004	309	534	EBOV-CP-Pat-012	198	177
EBOV-CP-Pat-004	365	352	EBOV-CP-Pat-012	290	432
EBOV-CP-Pat-004	389	636	EBOV-CP-Pat-013	201	222
EBOV-CP-Pat-004	429	506	EBOV-CP-Pat-013	216	233
EBOV-CP-Pat-005	188	1271	EBOV-CP-Pat-013	268	833
EBOV-CP-Pat-005	256	1173	EBOV-CP-Pat-013	326	495
EBOV-CP-Pat-005	362	374	EBOV-CP-Pat-013	374	482
EBOV-CP-Pat-005	362	375	EBOV-CP-Pat-013	395	243
EBOV-CP-Pat-005	384	555	EBOV-CP-Pat-013	425	234
EBOV-CP-Pat-005	384	340	EBOV-CP-Pat-014	77	115
EBOV-CP-Pat-006	137	1470	EBOV-CP-Pat-014	169	441
EBOV-CP-Pat-006	158	901	EBOV-CP-Pat-015	138	288
EBOV-CP-Pat-006	164	1078	EBOV-CP-Pat-015	229	425
EBOV-CP-Pat-006	200	1042	EBOV-CP-Pat-016	112	288
EBOV-CP-Pat-006	200	700	EBOV-CP-Pat-016	117	426
EBOV-CP-Pat-006	210	679	EBOV-CP-Pat-016	208	316
EBOV-CP-Pat-006	247	743	EBOV-CP-Pat-017	160	304
EBOV-CP-Pat-006	276	803	EBOV-CP-Pat-017	252	303
EBOV-CP-Pat-006	353	531	EBOV-CP-Pat-018	175	902
EBOV-CP-Pat-006	411	610	EBOV-CP-Pat-018	262	3418
EBOV-CP-Pat-006	438	466	EBOV-CP-Pat-018	330	1295
EBOV-CP-Pat-007	172	358	EBOV-CP-Pat-018	368	881
EBOV-CP-Pat-007	173	513	EBOV-CP-Pat-018	437	647
EBOV-CP-Pat-007	251	654	EBOV-CP-Pat-019	204	1283
EBOV-CP-Pat-007	382	2866	EBOV-CP-Pat-019	206	1106
EBOV-CP-Pat-008	228	366	EBOV-CP-Pat-019	211	1051
EBOV-CP-Pat-008	249	256	EBOV-CP-Pat-019	226	1156
EBOV-CP-Pat-008	288	388	EBOV-CP-Pat-019	226	840

902

Donor ID	DAYS FROM CONVALESCENCE	DABA au/ml	Donor ID	DAYS FROM CONVALESCENCE	DABA au/ml
EBOV-CP-Pat-019	259	1738	EBOV-CP-Pat-030	129	385
EBOV-CP-Pat-019	365	2636	EBOV-CP-Pat-030	145	455
EBOV-CP-Pat-019	402	1937	EBOV-CP-Pat-030	145	353
EBOV-CP-Pat-019	417	1753	EBOV-CP-Pat-030	166	402
EBOV-CP-Pat-019	465	1316	EBOV-CP-Pat-031	35	281
EBOV-CP-Pat-020	218	611	EBOV-CP-Pat-032	31	189
EBOV-CP-Pat-020	219	633	EBOV-CP-Pat-032	32	279
EBOV-CP-Pat-020	220	445	EBOV-CP-Pat-032	103	392
EBOV-CP-Pat-020	226	779	EBOV-CP-Pat-032	104	571
EBOV-CP-Pat-020	246	229	EBOV-CP-Pat-032	129	545
EBOV-CP-Pat-020	305	573	EBOV-CP-Pat-033	32	313
EBOV-CP-Pat-020	373	918	EBOV-CP-Pat-034	100	nd
EBOV-CP-Pat-020	417	643	EBOV-CP-Pat-035	217	189
EBOV-CP-Pat-020	432	557	EBOV-CP-Pat-036	48	105
EBOV-CP-Pat-020	480	781	EBOV-CP-Pat-036	82	83
EBOV-CP-Pat-021	218	677	EBOV-CP-Pat-037	240	1128
EBOV-CP-Pat-021	219	645	EBOV-CP-Pat-038	65	362
EBOV-CP-Pat-021	226	751	EBOV-CP-Pat-039	95	860
EBOV-CP-Pat-021	241	731	EBOV-CP-Pat-040	168	527
EBOV-CP-Pat-021	403	2853	EBOV-CP-Pat-041	179	365
EBOV-CP-Pat-021	430	2562	EBOV-CP-Pat-042	244	2453
EBOV-CP-Pat-021	467	1243	EBOV-CP-Pat-042	248	3161
EBOV-CP-Pat-021	484	1090	EBOV-CP-Pat-042	314	1645
EBOV-CP-Pat-021	505	865	EBOV-CP-Pat-042	332	958
EBOV-CP-Pat-022	215	141	EBOV-CP-Pat-043	179	317
EBOV-CP-Pat-022	219	276	EBOV-CP-Pat-043	238	388
EBOV-CP-Pat-022	325	235	EBOV-CP-Pat-044	95	308
EBOV-CP-Pat-023	45	159	EBOV-CP-Pat-045	186	602
EBOV-CP-Pat-023	115	513	EBOV-CP-Pat-045	242	523
EBOV-CP-Pat-024	185	691	EBOV-CP-Pat-045	256	296
EBOV-CP-Pat-024	108	543	EBOV-CP-Pat-045	270	454
EBOV-CP-Pat-025	115	698	EBOV-CP-Pat-045	293	3780
EBOV-CP-Pat-025	200	483	EBOV-CP-Pat-045	318	4235
EBOV-CP-Pat-026	85	439	EBOV-CP-Pat-045	340	3450
EBOV-CP-Pat-026	89	471	EBOV-CP-Pat-046	217	370
EBOV-CP-Pat-026	145	703	EBOV-CP-Pat-046	220	203
EBOV-CP-Pat-026	199	475	EBOV-CP-Pat-047	193	289
EBOV-CP-Pat-026	250	421	EBOV-CP-Pat-048	197	637
EBOV-CP-Pat-026	271	387	EBOV-CP-Pat-049	261	3624
EBOV-CP-Pat-026	332	328	EBOV-CP-Pat-049	262	3567
EBOV-CP-Pat-027	96	365	EBOV-CP-Pat-049	292	2430
EBOV-CP-Pat-027	173	468	EBOV-CP-Pat-049	313	2006
EBOV-CP-Pat-028	90	85	EBOV-CP-Pat-049	326	1517
EBOV-CP-Pat-028	156	275	EBOV-CP-Pat-049	345	1569
EBOV-CP-Pat-029	129	801	EBOV-CP-Pat-049	398	1184
EBOV-CP-Pat-029	213	379	EBOV-CP-Pat-050	180	618
EBOV-CP-Pat-029	243	557	EBOV-CP-Pat-051	193	929
EBOV-CP-Pat-029	291	491	EBOV-CP-Pat-052	225	816
EBOV-CP-Pat-029	291	416	EBOV-CP-Pat-052	262	431
EBOV-CP-Pat-029	315	381	EBOV-CP-Pat-052	282	541
EBOV-CP-Pat-030	31	243	EBOV-CP-Pat-052	302	686
EBOV-CP-Pat-030	32	126	EBOV-CP-Pat-052	325	699
EBOV-CP-Pat-030	104	350	EBOV-CP-Pat-052	352	668

903

Donor ID	DAYS FROM CONVALESCENCE	DABA au/ml
EBOV-CP-Pat-53	320	247
EBOV-CP-Pat-54	222	nd
EBOV-CP-Pat-055	130	213
EBOV-CP-Pat-055	236	649
EBOV-CP-Pat-056	82	315
EBOV-CP-Pat-057	160	183
EBOV-CP-Pat-057	254	346
EBOV-CP-Pat-058	166	948
EBOV-CP-Pat-058	256	592
EBOV-CP-Pat-059	142	319
EBOV-CP-Pat-059	238	487
EBOV-CP-Pat-060	48	nd
EBOV-CP-Pat-060	141	243
EBOV-CP-Pat-061	111	186
EBOV-CP-Pat-061	217	793
EBOV-CP-Pat-062	128	168
EBOV-CP-Pat-062	223	381
EBOV-CP-Pat-063	100	304
EBOV-CP-Pat-063	222	170
EBOV-CP-Pat-064	81	ndt
EBOV-CP-Pat-065	214	318
EBOV-CP-Pat-065	303	357
EBOV-CP-Pat-066	208	363
EBOV-CP-Pat-066	297	598
EBOV-CP-Pat-067	152	344
EBOV-CP-Pat-068	45	409
EBOV-CP-Pat-069	173	434
EBOV-CP-Pat-069	243	674
EBOV-CP-Pat-070	132	248
EBOV-CP-Pat-070	216	370
EBOV-CP-Pat-071	139	1308
EBOV-CP-Pat-071	153	1760
EBOV-CP-Pat-072	34	ndt
EBOV-CP-Pat-073	129	431
EBOV-CP-Pat-073	213	179
EBOV-CP-Pat-074	308	1412
EBOV-CP-Pat-075	322	533
EBOV-CP-Pat-076	136	606
EBOV-CP-Pat-077	246	371
EBOV-CP-Pat-078	260	443
EBOV-CP-Pat-079	245	590
EBOV-CP-Pat-080	262	314
EBOV-CP-Pat-081	172	642
EBOV-CP-Pat-082	245	1153
EBOV-CP-Pat-083	254	708
EBOV-CP-Pat-084	142	528
EBOV-CP-Pat-084	243	486
EBOV-CP-Pat-085	290	725
EBOV-CP-Pat-086	297	484
EBOV-CP-Pat-087	302	363
EBOV-CP-Pat-088	285	410
EBOV-CP-Pat-089	56	nd
EBOV-CP-Pat-090	262	665
EBOV-CP-Pat-091	239	1452
EBOV-CP-Pat-092	297	525
EBOV-CP-Pat-093	220	1334
EBOV-CP-Pat-094	238	805
EBOV-CP-Pat-095	275	1176
EBOV-CP-Pat-096	275	318
EBOV-CP-Pat-097	277	560
EBOV-CP-Pat-098	277	356
EBOV-CP-Pat-099	227	578
EBOV-CP-Pat-100	270	1131
EBOV-CP-Pat-101	210	783
EBOV-CP-Pat-102	277	1684
EBOV-CP-Pat-103	240	492
EBOV-CP-Pat-104	293	834
EBOV-CP-Pat-105	267	382
EBOV-CP-Pat-106	213	513
EBOV-CP-Pat-107	220	420
EBOV-CP-Pat-108	219	468
EBOV-CP-Pat-109	219	3394
EBOV-CP-Pat-110	237	598
EBOV-CP-Pat-111	246	725
EBOV-CP-Pat-112	283	741
EBOV-CP-Pat-113	276	383
EBOV-CP-Pat-114	211	339
EBOV-CP-Pat-115	208	347

nd =Not Detected

904

Supplementary Table 2 Alignment of the glycoprotein amino acid sequence of the three isolates, pEBOV14-GP, pEBOV14m-GP and pEBOV95-GP used in the study, aligned to the reference strain KJ669348. The linear and conformational epitopes affecting antibody neutralization are indicated below the sequence, each colour corresponding to a different epitope. All glycoprotein regions are color-coded above the sequences. The black bars indicate N-linked potential glycan positions.

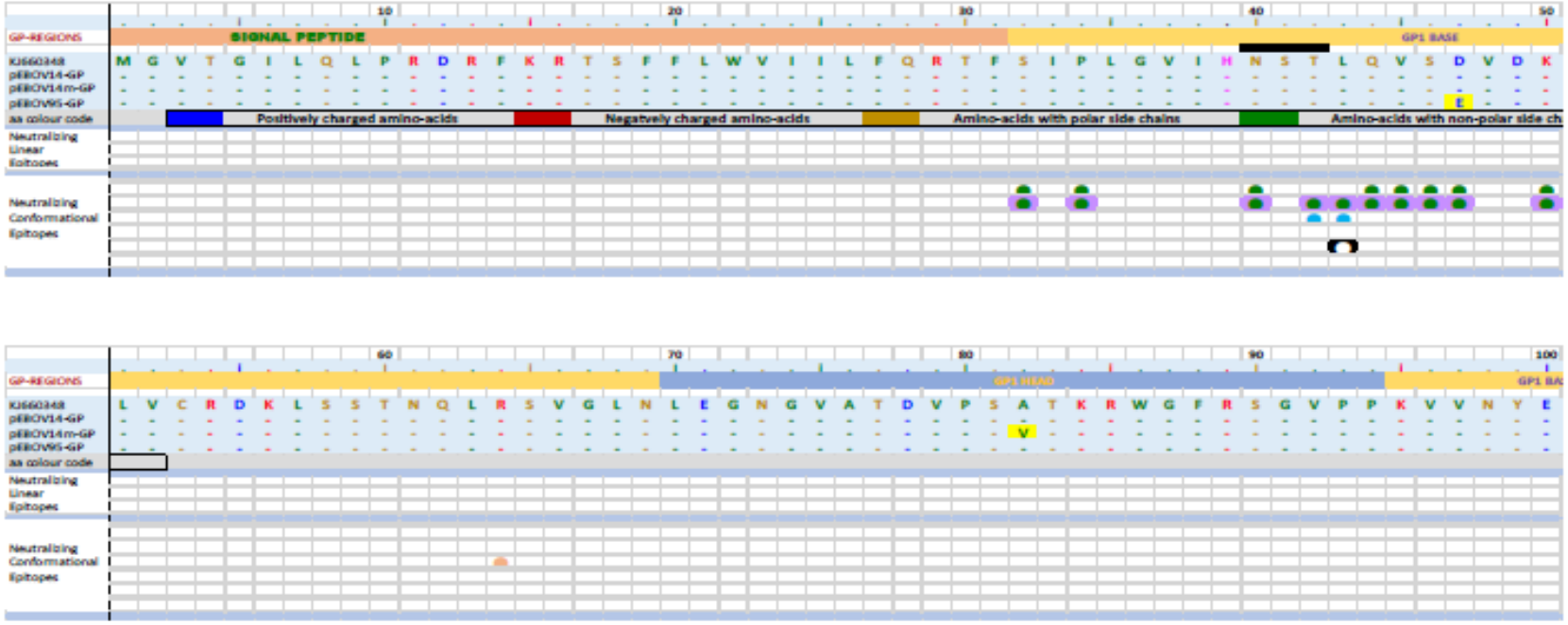

905

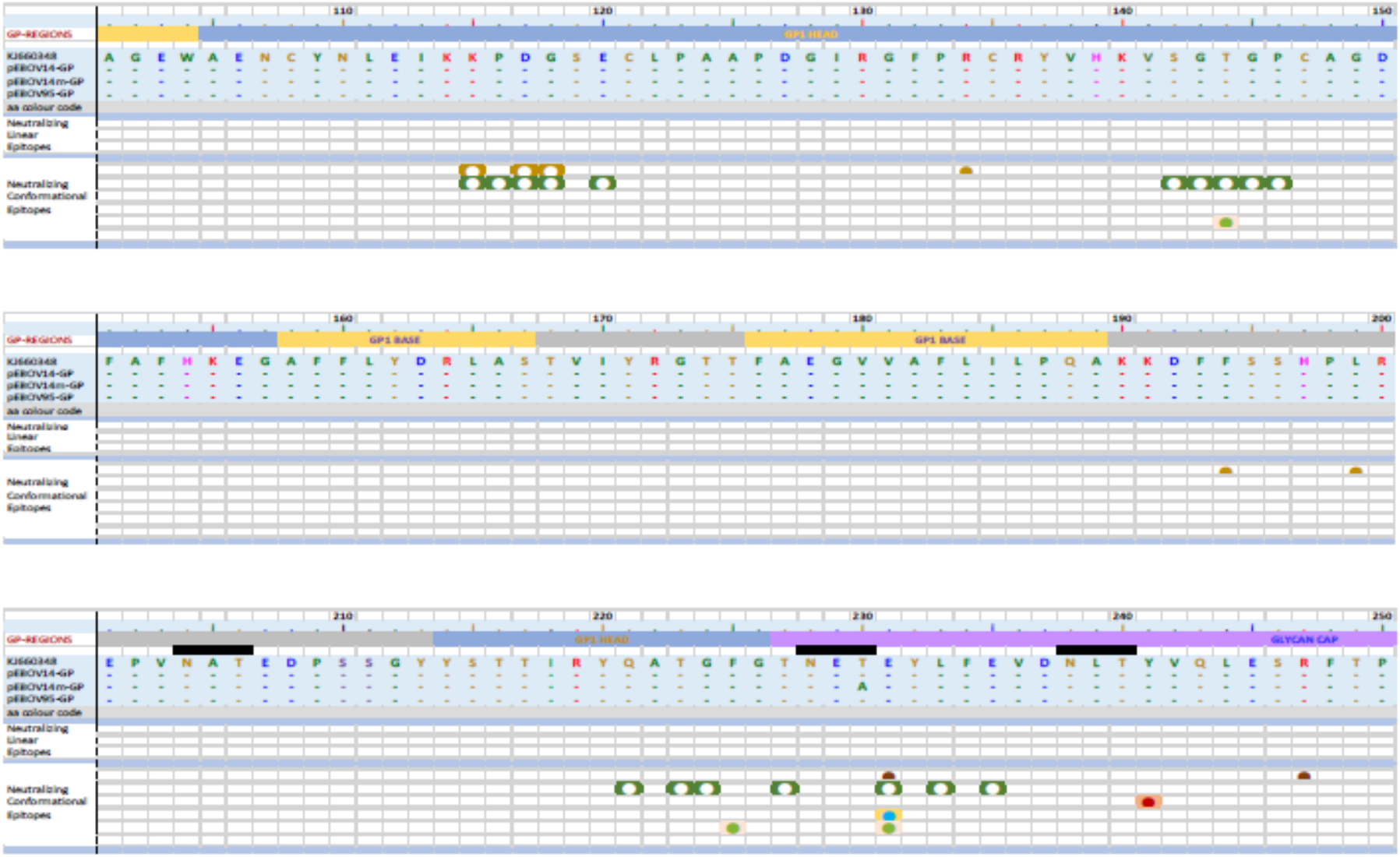
110
120
130
140
150
GP-REGIONS
GP1 HEAD
KJ660348
pEBOV14-GP
pEBOV14m-GP
pEBOV9S-GP
aa colour code
Neutralizing
Linear
Epitopes
Neutralizing
Conformational
Epitopes
160
170
180
190
200
GP1 BASE
GP1 BASE
210
220
230
240
250
GP1 HEAD
GLYCAN CAP


GP-REGIONS
KJ660348
pEBOV14-GP
pEBOV14m-GP
pEBOV9S-GP
aa colour code
Neutralizing Linear Epitopes
Neutralizing Conformational Epitopes
MUCIN LIKE DOMAIN

907

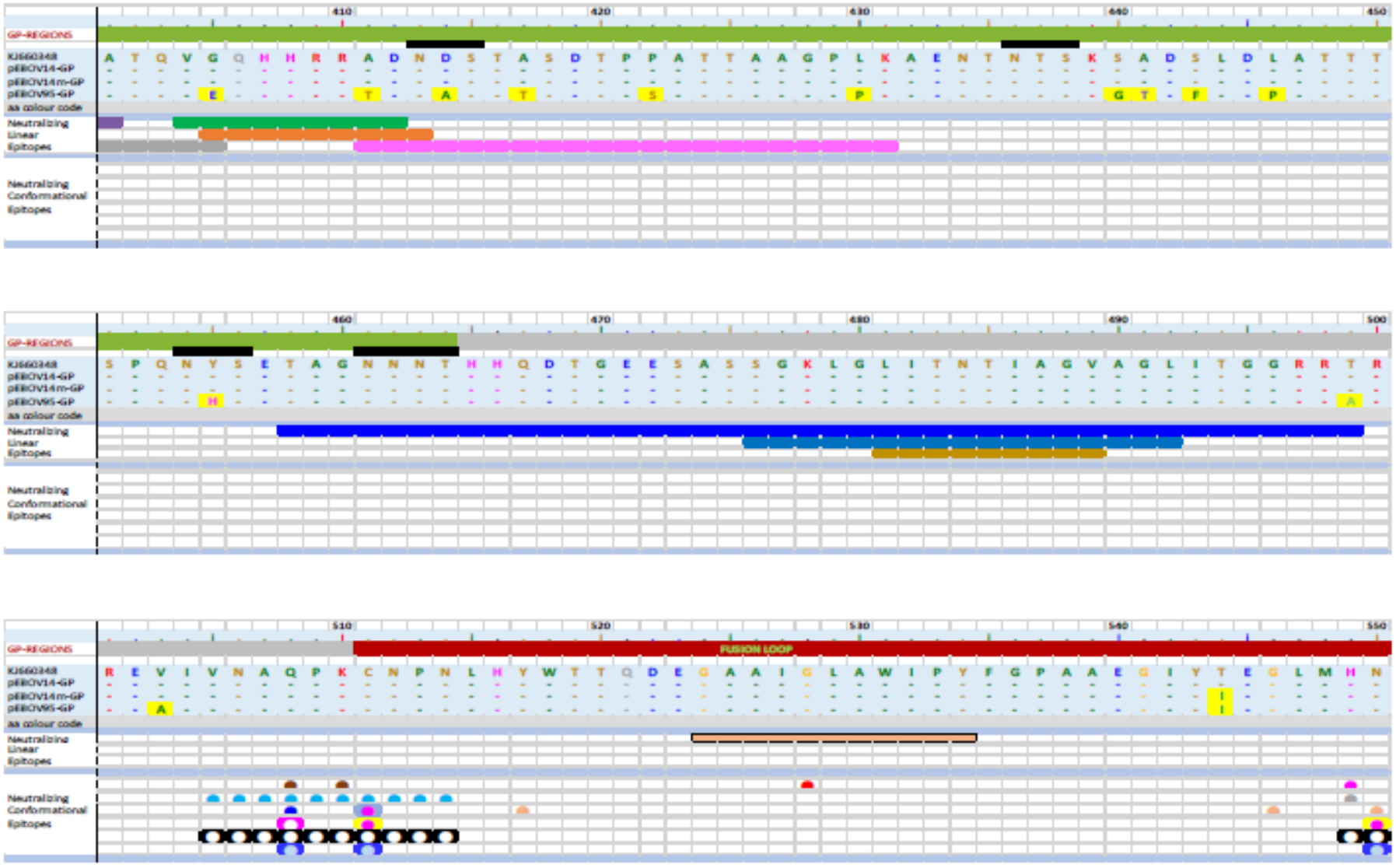
GP-REGIONS
KJ660348
pEBOV14-GP
pEBOV14m-GP
pEBOV9S-GP
aa colour code
Neutralizing
Linear
Epitopes
Neutralizing
Conformational
Epitopes
FUSION LOOP

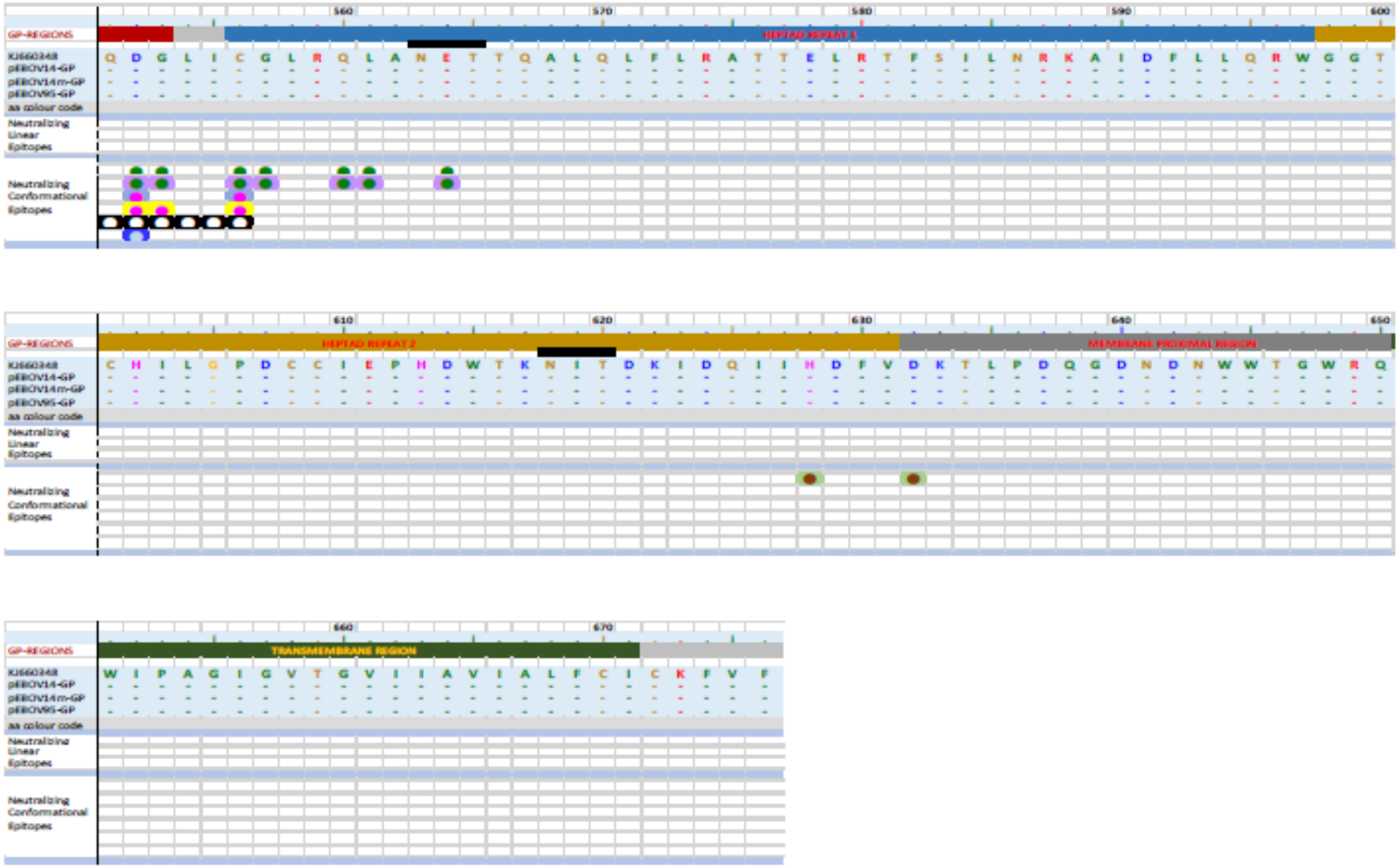
560
570
580
590
600
GP-REGIONS
HEPTAD REPEAT 1
KJ660348
pEBOV14-GP
pEBOV14m-GP
pEBOV9S-GP
aa colour code
Neutralizing Linear Epitopes
Neutralizing Conformational Epitopes
610
620
630
640
650
HEPTAD REPEAT 2
MEMBRANE PROXIMAL REGION
660
670
TRANSMEMBRANE REGION

909

Supplementary Table 2 continued: Epitope colour code as indicated in the alignement.

 **R64, Y517, G546, N550** Discontinuous epitope (epitope ID 857744) studied as part of Envelope glycoprotein from Zaire ebolavirus. (Cell. 2017 169(5):891-904.e15).

 **R134, F194, L199** Discontinuous epitope (epitope ID 149583) studied as part of Envelope glycoprotein from Zaire ebolavirus. [226/8.1] (J Virol. 2003 77(2):1069-74).

 **Q508** Discontinuous epitope (epitope ID 234005) studied as part of Envelope glycoprotein from Zaire ebolavirus. (Sci Rep. 2014 4:6881).

 **G528** Discontinuous epitope (epitope ID 434700) studied as part of Envelope glycoprotein from Zaire ebolavirus. (Cell. 2017 169(5):878-890).

 **C511, D552, C556** is a discontinuous epitope (epitope ID 442028) studied as part of Envelope glycoprotein from Zaire ebolavirus. (J Virol. 2015 89(21):10982-92).

 **C511, N550, D552, G553, C556** Discontinuous epitope (epitope ID 442029) studied as part of Envelope glycoprotein from Zaire ebolavirus. (J Virol. 2015 89(21):10982-92).

 **Chain I: S32, P34, N40, E44, V45, T46, E47; Chain J: N552, A553, C556, G557, Q560, L561, E564** Discontinuous epitope (epitope ID 167710) studied as part of Envelope glycoprotein from Sudan ebolavirus. [Ab:16F6] (Viruses. 2012 4(4):447-70).

 **Chain I: S32, P34, N40, T42, L43, E44, V45, T46, E47, Q50; Chain J: N552, A553, C556, G557, Q560, L561, E564.** Discontinuous epitope (epitope ID 164107) studied as part of Envelope glycoprotein from Sudan ebolavirus. (Nat Struct Mol Biol. 2011 18(12):1424-7).

 **R64, Y517, G546, N550** Discontinuous epitope (epitope ID 857744) studied as part of Envelope glycoprotein from Zaire ebolavirus. (Cell. 2017 169(5):891-904).

 **K115, D117, G118** Discontinuous epitope (epitope ID 538601) studied as part of Envelope glycoprotein from Zaire ebolavirus. (Cell Rep. 2016 15(7):1514-1526).

 **H549** Discontinuous epitope (epitope ID149582) studied as part of Envelope glycoprotein from Zaire ebolavirus. [133/3.16] (J Virol. 2003 77(2):1069-74).

 **C511, D552, C556** Discontinuous epitope (epitope ID 442028) Studied as part of Envelope glycoprotein from Zaire ebolavirus. (J Virol. 2015 89(21): 10982–10992).

 **L43, V505, N506, A507, Q508, P509, K510, C511, N512, P513, N514, H549, N550, Q551, D552, G553, L554, I555, C556.** Discontinuous epitope (epitope ID530633) studied as part of Envelope glycoprotein from Zaire ebolavirus. (Nature. 2008 454(7201):177-82).

 **L273, W275** is a discontinuous epitope (epitope ID 503951) Studied as part of spike glycoprotein from Bundibugyo ebolavirus. (Cell. 2016 164(3):392-405).

 **E231, R247, L254, G271, K272, P279.** Discontinuous epitope (epitope ID 606555) studied as part of Envelope glycoprotein from Zaire ebolavirus. (Cell. 2017 169(5):878-890).

 **Y241, W275** Discontinuous epitope (epitope ID 503953) studied as part of spike glycoprotein from Bundibugyo ebolavirus. (Cell. 2016 164(3):392-405).

910

 **K114, K115, P116, D117, G118, E120, S142, G143, T144, G145, P146, Q221, T223, G224, T227, E231, L233, Y241, T269.** Discontinuous epitope (epitope ID 534854) studied as part of Envelope glycoprotein from Zaire ebolavirus. (Science. 2016 351(6279):1343-6).

 **E231, T270, W275.** Discontinuous epitope (epitope ID 539005) studied as part of Envelope glycoprotein from Zaire ebolavirus. (Sci Rep. 2016 6:25856).

 **Q508, C511, N550, D552** Discontinuous epitope (epitope ID 539006) studied as part of Envelope glycoprotein from Zaire ebolavirus. (Sci Rep. 2016 6:25856).

 **T144, E231, W275** Discontinuous epitope (epitope ID 539007) studied as part of Envelope glycoprotein from Zaire ebolavirus. (Sci Rep. 2016 6:25856).

 **H628, D632** Discontinuous epitope (epitope ID 606557) studied as part of Envelope glycoprotein from Zaire ebolavirus. (Cell. 2017 169(5):878-890).

 **L274, Q508** are mutations confering resistance to ZMAb. (Sci Rep. 2014; 4: 6881).

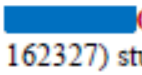 **GKLGLITNTIAGVAGLI [aa 477-493]** Linear peptidic epitope (epitope ID 162327) studied as part of Envelope glycoprotein from Zaire ebolavirus. [14G7] (Cell Rep. 2018 24(4):1050-1059.e5)(J Virol. 2012 86(5):2809-16)(Science. 2000 287(5458):1664-6).

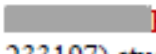 **HNTPVYKLDISEATQVE[aa 389-405]** Linear peptidic epitope (epitope ID 233197) studied as part of Envelope glycoprotein from Zaire ebolavirus. (Science. 2000 287(5458):1664-6).

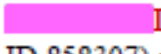 **DNDSTASDTPPATTAAGPLK [aa 401 431]** Linear peptidic epitope (epitope ID 858307) studied as part of Envelope glycoprotein from Zaire ebolavirus. (Cell Physiol Biochem. 2018;50(3):1055-1067).

 **AGNNNTHHQDTGEESASSGKLGLITNTIAGVAGLITGGRRTR [aa 459-500]** Linear peptidic epitope (epitope ID 156605) studied as part of Envelope glycoprotein from Zaire ebolavirus.(Cell Rep. 2018 24(4):1050-1059)(J Virol. 2012 86(5):2809-16)(Science. 2000 287(5458):1664-6.

 **EQHHRRTDN [aa 405-413]** Linear peptidic epitope (epitope ID 13837) studied as part of Envelope glycoprotein from Zaire ebolavirus.(Proc Natl Acad Sci U S A. 2014 111(48):17182-7.

 **VEQHHRRTD [aa 404-412]** Linear peptidic epitope (epitope ID 68320) studied as part of Envelope glycoprotein from Zaire ebolavirus. (J Mol Biol. 2008 375(1):202-16.

 **VYKLDISEA [aa 393-401]** Linear peptidic epitope (epitope ID 72065) studied as part of Envelope glycoprotein from Zaire ebolavirus. (Cell Rep. 2018 24(4):1050-1059.

 **LITNTIAGV [aa 481-489]** Linear peptidic epitope (epitope ID 36729) studied as part of Envelope glycoprotein from Zaire ebolavirus. (PLoS Curr. 2014 6: ecurrents outbreaks).

 **GEWAF [aa 286-290]** (J Virol. 2016 90(1): 279–291).

911

Supplementary Table 3a Rationale for selection of DABA antibody stimulation structural models. -2LL, AIC and BIC values for exponential growth and logistic growth structural models. As discussed in Mould et al. 2013 Pharmacometrics & Systems Pharmacology (2013) 2, e38 there is "positive to strong evidence" (ΔBIC > 6-10) for the logistic growth structural model with a drop of 5.93 in BIC. In practice, a drop in AIC or BIC of 2 is often a threshold for considering one model over another.

Structural Model	Objective Function		
	-2LL	AIC	BIC
Exponential growth	784.37	790.82	796.5
Logistic Growth	778.44	784.89	790.57

Supplementary Table 3b Rationale for selection of DABA antibody decay structural models. -2LL, AIC and BIC values for one and two compartment decay. As discussed in Mould et al. 2013 Pharmacometrics & Systems Pharmacology (2013) 2, e38 there is "strong to very strong evidence" (ΔBIC >10) for the "2 compartment decay model with saturable recycling" structural model with drops in BIC of 54.84, 27.29 and 9.89 in comparison to the one compartment, one compartment with saturable recycling and two compartment decay structural models. In practice, a drop in AIC or BIC of 2 is often a threshold for considering one model over another.

Structural Model	Objective Function		
	-2LL	AIC	BIC
One compartment decay	991.89	998.23	1004.85
One compartment decay with saturable recycling	960.03	968.6	977.3
Two compartment decay	942.63	951.2	959.9
Two compartment decay with saturable recycling	924.1	937.34	950.01

912

Supplementary Table 3c – Credibility intervals for selected DABA antibody stimulation and decay structural models at a 95% confidence level. Values generated via Monte Carlo simulation to create 1000 x npoint samples with replacement from the weighted marginal distribution of each parameter, where npoint is the number of support points in the model.

Model Parameters	Credibility Intervals
Logistic Growth	
k_{growth}	0.012 – 0.040
K_{max}	649.71 – 5287.24
2 compartment decay with recycling	
V_{max}	3.24 – 24.42
K_m	377.17 – 1971.13
k_{end}	0.0086 – 0.021
k_{cp}	0.017 – 0.97
k_{pc}	5.57 – 6.86

The credibility intervals (at a 95% confidence level) do not overlap with zero and are relatively tight, given the variability of the data. These are not of concern as this reflects the contribution of these parameters for different individual stimulation and decay profiles. All the above metrics indicate that the models were identifiably the best models tested.

913

Supplementary Table 4 Fitted population parameters for IgG restimulation and decay compartmental models. k_{growth} and K_{max} are first order rate constants for restimulation and maximum IgG carrying capacity parameters for the 1-compartment saturable stimulation model, respectively. Parameters for the 2-compartment decay model with saturable recycling V_{max}, K_m and k_{end} denote the maximum recycling rate, Michaelis Menten constant and endogenous decay rate for IgG, respectively. k_{pc} and k_{pc} denote the first order rate constants to and from the peripheral compartment for the 2-compartment decay model with saturable recycling, respectively.

Assay	1-compartmental saturable stimulation model				2-compartment decay model with saturable recycling									
	k_{growth}		K_{max}		V_{max}		K_m		k_{end}		k_{cp}		k_{pc}	
	mean	%CV	mean	%CV	mean	%CV	mean	%CV	mean	%CV	mean	%CV	mean	%CV
DABA	0.03	115.30	2925.60	77.10	15.40	68.30	979.00	75.20	0.03	127.80	0.93	103.00	6.20	18.00
EBOV14 Neut	0.07	6.20	186.50	32.10	16.80	54.90	1340.50	43.10	0.03	74.80	0.85	116.50	5.20	59.60
EBOV95 Neut	0.05	72.90	387.10	23.20	7.00	45.10	235.30	37.30	0.03	28.90	1.53	75.60	11.10	61.50

914

915